Supplementary Materials for

Conservation, acquisition, and functional impact of sex-biased gene expression in mammals

Sahin Naqvi, Alexander K. Godfrey, Jennifer F. Hughes, Mary L. Goodheart, Richard N. Mitchell, David C. Page*

*Corresponding author. Email: dcpage@wi.mit.edu

Published 19 July 2019, *Science* **365**, eaaw7317 (2019)
DOI: 10.1126/science.aaw7317

This PDF file includes:

Materials and Methods
Figs. S1 to S26
Tables S3 and S8
Captions for Tables S1, S2, S4 to S7, and S9
References

Other Supplementary Material for this manuscript includes the following:
(available at science.sciencemag.org/content/365/6450/eaaw7317/suppl/DC1)

Tables S1, S2, S4, S6, and S9 (.xlsx)
Tables S5 and S7 (.txt)

Materials and Methods

Selection of human (GTEx) samples

We considered the following tissues as described in GTEx terminology: skin (not sun-exposed), heart – left ventricle, muscle – skeletal, brain – cortex, spleen, adipose – visceral (omentum), thyroid, colon – transverse, lung, liver, pituitary, and adrenal gland. RNA-seq samples from each of these tissues were first subjected to a series of filters based on sample-level quality metrics and individual-level medical history and cause of death. At the sample level, we excluded samples if they met any of the following criteria: flagged by GTEx (SMTORMVE = FLAGGED), RNA integrity number (SMRIN) less than 6.0, or autolysis score (SMATSSCR) greater than 2. At the individual level, all samples from an individual were excluded if the individual met any of the following criteria: Hardy scale death classification (DTHHRDY) of 4 (slow death), died of metabolic acidosis or shock (DTHCAT), greater than 72 hours on a ventilator prior to death (DTHVNTD), medical history of any of the following: ascites (MHASCITES), lupus (MHLUPUS), Reyes Syndrome (MHREYES), scleroderma (MHSCLRDRM), or sarcoidosis (MHSRCDSS). For a number of additional medical histories and causes of death, samples from specific subsets of tissues from an individual were excluded. The details of this filtering are provided in the provided supplementary code.

We next evaluated notes on sample histology provided by GTEx in order to eliminate samples with grossly skewed cell-type proportions or other significant pathologies. The exclusionary criteria for each tissue as well as the list of GTEx samples passing all of the above-described filtering steps are provided in Table S1.

Detailed histological evaluation of GTEx samples

For a subset of tissues, we performed detailed additional histological evaluation of all GTEx samples that passed the filters described above, with the goal of ensuring that male and female samples were histologically comparable. Samples were evaluated by a single pathologist (RM), without knowledge of age or sex. Evaluations were based on low- to high-power scans of hematoxylin and eosin-stained tissues as downloaded from the GTEx website and performed in one or two sittings. Adipose tissue (visceral omentum) was evaluated for the percentage of the sample that was either connective tissue or vasculature, as opposed to pure adipocytes. Adrenal gland was assessed for general preservation (degree of autolysis), content of fibrosis, whether there was medulla present or not, and the extent of any associated mononuclear cell infiltrate. Liver was evaluated on a qualitative scale of 0-3 for the degree of vascular congestion, 0-3 for the extent of periportal mononuclear cell infiltrate, the percentage of fibrosis in the sample (relative to hepatocytes), the presence of the capsule, and the extent of steatosis. Muscle (skeletal) was assessed on a qualitative scale of 0-3 for the extent of fibrosis and adipose tissue, and whether there was myocyte atrophy present (none/focal/multifocal). Spleen was evaluated for the percentage of connective tissue, the amount of white pulp (low, average, increased), and the presence of extramedullary hematopoiesis (none/focal/multifocal). Thyroid was evaluated on a qualitative scale of 0-3 for the extent of interstitial fibrosis and 0-3 for mononuclear cell infiltrate. In general, there were no significant differences between male and female samples with respect to these histological evaluations (Table S2). Exceptions were the percentage of connective tissue/vasculature in adipose tissue and the degree of interstitial fibrosis in thyroid; we adjusted for these differences in downstream analyses.

Sample collection for non-human mammals

Cynomolgus macaque samples were collected from a breeding colony in Mauritius (Noveprim). Dog samples were collected from a beagle breeding facility in Wisconsin (Rigdlan Farms). Mouse and rat samples were collected from the C57/BL6J (Jackson Labs; stock 000664) and Brown Norway (Charles River; strain code 091) strains, respectively. All animal work was approved by the Animal Care and Use Committee at the Massachusetts Institute of Technology (protocol #0617-059-20). Age ranges for each species were as follows: cyno, 72-107 months; dog, 19-37 months; mouse, 8 weeks; rat, 9 weeks. Female macaques and dogs in estrus phase were excluded based on visual inspection prior to tissue isolation. Vaginal swabs were performed on female mice and rats at the time of tissue collection, and estrous phase was assessed post-mortem by Diff-Quick Stain Kit (Thermo Fisher). Enough females were collected such that tissues from three non-estrus females were available after post-mortem assessment of estrous phase. All tissues were isolated from freshly sacrificed animals (< 1 hour from time of death to tissue fixation). In order to render data from the non-human mammals maximally comparable to RNA-seq from human tissues from GTEx, we adapted the GTEx Tissue Harvesting Work Instruction (PR-0004-W1, available at https://biospecimens.cancer.gov/resources/sops/library.asp) to each species, sampling the same part of the tissue as GTEx (the specific list of GTEx tissues for which the protocol was adapted is provided in the "Selection of human (GTEx) samples" section). Tissues were washed in cold PBS and stored in RNALater (Ambion) per the manufacturer's instructions.

Library construction and sequencing

RNAs were extracted and sequencing libraries prepared in independent batches, with batch assignments randomized with respect to tissue, sex, and species. Technical replicates from each species were included in each library preparation and sequencing batch. Testis samples were used for technical replicates as the testis is among the most transcriptionally complex organs, allowing us to assess the impact of batch on the expression of the greatest number of genes. Sequencing libraries were prepared using the TruSeq mRNA library kit (Illumina) according to manufacturer's instructions with the following modifications: After prep, libraries were size-selected using 2% agarose gels on the PippinHT system (Sage Science) with a capture window of 300-600 bases. The size-selected material was then subjected to one additional cycle of PCR with fresh reagents and P5/P7 primers (Illumina) to ensure all library fragments were fully double-stranded. This step significantly reduced the percentage of smaller fragments co-purifying in the final gel size-selection. After PCR, libraries were size-selected a second time on the PippinHT with the same settings, and the resulting libraries were sequenced for either 100x100 or 75x75 cycles on an Illumina HiSeq 2500 sequencer. We sequenced a subset of samples with high coverage and longer reads ($\geq 10^8$ paired-end reads, 100 bp x100 bp), and the remainder with moderate coverage and shorter reads ($\geq 3 \times 10^7$ paired-end reads, 75 bp x75 bp).

Read mapping and analysis

RNA-seq libraries from the non-human mammals were mapped to their respective reference genomes (cyno, macFas5; dog, canFam3; mouse, mm10; rat, rn6) using STAR (*82*) v2.5.0 with the following parameters: --outFilterMultimapNmax 50 --outFilterMismatchNmax 999 --outFilterMismatchNoverReadLmax 0.15. For cynomolgus macaque, we generated a custom assembly of the Y chromosome by aligning whole-genome sequencing data (study SRP045278;

runs SRR1564773, SRR1564774, SRR1564776, SRR1564777) to our published assembly of the Y chromosome of the closely related rhesus macaque (*83*) using bowtie (*84*) v1.1.1 with default parameters, and manually verifying and correcting substitutions using Consed (*85*). StringTie (*86*) v1.3.3b with the --rf parameter was run on each resulting .bam file to assemble novel isoforms relative to the reference transcriptome annotation (Ensembl 91 for cyno; Ensembl 84 for dog, mouse, and rat). The sets of novel and existing transcript annotations from each library were then compiled into a single set of annotations for each species using the --merge option in StringTie. Abundances for these sets of transcripts for each species were then quantified using salmon (*87*) v0.9.1 with the following parameters/flags: --seqBias, --gcBias, --useVBOpt. For human samples from GTEx, transcript abundances for GENCODE v26 annotations were quantified using salmon with the same parameters.

Removal of samples identified as expression outliers

To remove expression outliers in the human GTEx dataset, we calculated, for each tissue, the pairwise Pearson correlation r_{ij} between samples *i* and *j*, on log-transformed TPM values for all genes. The typical relatedness of sample *i* to other samples in that tissue is $\overline{r_i} = \mathrm{median}_j(r_{ij})$. We then express this relatedness in median absolute deviations as

$$D_i = |\overline{r_i} - \bar{\bar{r}}| / \operatorname*{median}_j(|\overline{r_j} - \bar{\bar{r}}|)$$

where $\bar{\bar{r}}$ is the grand correlation median. Across the 12 tissues, 53 samples with $D > 6$ were marked as outliers and removed from subsequent analyses. To remove expression outliers in the non-human mammals, we performed hierarchical clustering of all samples within each species based on pairwise Pearson correlations of log-transformed TPM values. Samples that did not cluster clearly with all other samples of the same tissue and were verified to not be label swaps

were marked as expression outliers. Across the 12 tissues and four non-human mammals, 15 out of 292 samples were marked as outliers and removed from subsequent analyses.

Gene expression calculation and clustering

The tximport R package (*88*) (with countsFromAbundance = "lengthScaledTPM") was used to sum transcript-level counts and transcripts per million (TPM) values from salmon to the gene level. Jensen-Shannon divergence between counts per million (CPM) values was used as a measure of sample distance, and average-linkage hierarchical clustering was used to cluster samples. First, samples within each species were clustered. Next, gene counts from all five species (all non-human mammal samples, as well as six random human samples per tissue) were collected into a single matrix on the basis of one-to-one orthologs. We relied upon orthology information from Ensembl 91, manually adding orthology information from X- and Y-linked genes *DDX3X/DDX3Y*, *ZFX/ZFY*, *KDM6A/UTY*, *KDM5C/D*, and *USP9X/USP9Y*. Gene-level counts across all samples were normalized using the TMM method implemented in the edgeR (*89*) package, and normalized resulting CPM values were used for clustering as in Figure 1b.

Principal components analysis to adjust for hidden confounders

For human samples, principal components (PCs) analysis within each tissue was performed on the gene x sample matrix of residual CPM values after first subtracting the mean effect of sex. We chose the number of PCs to adjust for by picking the smallest number of PCs after which the marginal gain in percent variance explained began to decrease. The chosen number of PCs ranged between two and four for all 12 tissues. Within each tissue, a limma/voom linear model

consisting of the selected PCs was then constructed, and the residuals of this model were used as adjusted expression values. These adjusted expression values were then combined with data from the additional species for downstream clustering and differential expression analyses.

Estimation of relative cell-type proportions in bulk tissue samples

We used CIBERSORT version 1.04 (https://cibersort.stanford.edu) to estimate relative cell-type proportions in human brain, skin, and adipose, three tissues where reference datasets of pure tissue-resident cell populations were readily accessible. For each tissue, we input the (unadjusted by PCA) gene x sample TPM matrices. To estimate relative cell-type proportions from these samples, CIBERSORT requires gene expression profiles of reference cell-types expected to make up the tissue, from which it derives a "signature matrix" consisting of genes that most accurately differentiate the cell-types. For brain, we used FPKM estimates in five adult cell-types (astrocytes, oligodendrocytes, neurons, microglia, endothelial cells) from Zhang et al (http://web.stanford.edu/group/barres_lab/brainseq2/TableS4-HumanMouseMasterFPKMList.xlsx) (*90*). For skin, we used FPKM estimates in three cell types (keratinocytes, fibroblasts, melanocytes) from Reemann et al (*91*). For adipose, we constructed the signature matrix as described in Glastonbury et al (*92*).

Linear modeling and differential expression

Linear modeling was performed using the limma R package, with the voom functionality for analyzing RNA-seq read counts (*78*). Within each tissue, we assessed one-to-one orthologs with mean TPM greater than 1 in at least four of the five species. This resulted in a range of 8,166 (muscle) to 10,449 (pituitary) orthologs assessed in each tissue (across all species), with 12,013

orthologs assessed in at least one of the 12 tissues. To detect sex bias conserved across the majority of species, we modeled expression (TMM-normalized CPM values) within each tissue as a linear function of species and sex. A challenge in modeling sex across multiple species is that the species differ in both sample size and variability, with a greater number of human samples that also exhibit greater variability. To control for between-species differences in sample size and variability, we applied a linear mixed model (LMM) approach, in which species was specified as the random effect, using the limma's duplicateCorrelation function, specifying species as the block variable. We used the voomWithQualityWeights (*93*) function to estimate group-specific variances. P-values from all assessed gene-tissue pairs were adjusted using the qvalue method (*94*). To empirically estimate the false discovery rate for the LMM approach, we permuted the male/female sample labels within each tissue/species combination and used the qvalue method to obtain $1-\pi_0$, or the proportion of "true" p-values across all gene-tissue pairs. In order for a gene-tissue pair to be ultimately classified as showing conserved sex bias, we required that the LMM for that gene-tissue pair yielded a qvalue < 0.1, and that the gene-tissue pair also show a $\geq$ 1.05 fold-change magnitude, as determined by linear regression in each species separately, in the same direction in at least four of the five species. To validate the results of the LMM, we performed linear regressions for sex within each of the 60 tissue-species combinations using limma/voom, and ranked all expressed genes within each tissue-species combination by –log10(p-value) from the linear regression, signed by the direction of sex bias (male-biased as positive, female-biased as negative). Within each tissue, we then computed the median of this rank statistic across the five species. In this way, genes in a given tissue showing relatively low p-values and male-biased expression consistently across species would have high

rankings, while genes with consistently low p-values and female-biased expression would have low rankings.

To assess lineage-specific sex bias, we performed linear regressions for sex within each of the 60 tissue-species combinations using limma/voom. The effect size estimates for sex and the corresponding standard errors from each tissue-species combination were then combined into a 12,013 x 60 matrix. Missing values (i.e., orthologs not expressed in a particular gene-tissue combination) were set to an effect size of 0 and a standard error of 1000. Mashr (*46*) performs Empirical Bayes-based shrinkage on effect size estimates while learning patterns from the data, and works optimally when provided with broad trends in effect sizes, upon which it performs additional refinements. To this end, we performed sparse factor analysis (SFA) (*95*) on the 12,013 x 60 matrix of ortholog Z-scores (effect size divided by standard error) with default parameters. The learned sparse factors were then converted into 60x60 covariance matrices, combined with canonical covariance matrices and covariance matrices learned using PCA, and input to the main mash function along with the effect size and standard error estimates. Within each of the 60 tissue-species combinations, we called sex-biased genes with mashr local false sign rate $\leq$ 5%, and estimated posterior mean fold-change $\geq$ 1.05. Within each tissue, we assigned the lineage of gain or loss of sex bias based on parsimony when considering the five species. Genes sex-biased in only one of the five species were assigned as species-specific gains. Genes sex-biased in the same direction in both human and cyno or in both mouse and rat were assigned as gains in the primate or rodent lineages, respectively. Genes sex-biased in the same direction in human, cyno, and dog were assigned as losses in the rodent lineages, while those sex-biased in mouse, rat, and dog were assigned as losses in the primate lineage. The most parsimonious explanation for genes sex-biased in the same direction in one primate species

(human or cyno) and one rodent species (mouse or rat) is two independent gains of sex bias in each lineage. Similarly, genes sex-biased in the same direction in exactly one primate, exactly one rodent, and in dog are most consistent with two independent losses of sex bias. The remainder of cases were assigned as "complex". In order to obtain empirical estimates of false discovery rates for each of the 10 evolutionary classes of sex bias, we permuted the sample labels for sex within each tissue and repeated the above analyses. We used the results of this analysis with permuted sample labels to calculate the FDR at two levels: 1) for all sex-biased gene-tissue pairs of a given evolutionary class, regardless of tissue (i.e. Fig. 3), and 2) for each tissue separately, an estimate of the number of genes belonging to each evolutionary class of sex bias and an FDR for the number of genes in each class, which are provided in Table S4 and which we used when performing the motif enrichment analyses described below.

Estimates of sex bias in independent datasets

Transcript counts and abundances were quantified using RNA-seq reads from Liang et al (*27*) (human skin, GSE63980), Lindholm et al (*40*) (human muscle, GSE58387 and GSE59608), Li et al (*44*) (mouse liver, muscle, heart, lung, spleen, adrenal, PRJNA375882), Marin et al (*43*) (mouse liver, heart, GSE97367), and Seo et al (*61*) (cattle pituitary gland, GSE65125). Raw read (fastq) files were input to salmon, supplying either the human or mouse transcriptome annotations described above or cattle transcriptome annotations from Ensembl v91. Sex bias in each dataset was estimated by linear regression in limma/voom. Since Lindholm et al sampled multiple muscle regions from the same individual, limma's linear mixed model approach was used to specify individual as a random effect and sex as a fixed effect. For mouse liver and heart, data from both Li et al and Marin et al were combined, and the effect of sex was estimated while

specifying the study as a covariate. Sex bias in microarray data from Yang et al (*19*) and Franco et al (*45*) (mouse muscle, GSE3088, and lung, GSE16510, respectively) was analyzed using NCBI's GEO2R tool. Genes with FDR < 0.1 (as determined by the qvalue method) in these studies were considered significant; for these genes, the male/female fold-changes between the published study and our study were compared. When raw data were not publicly available, estimates for significantly sex-biased genes calculated in each study were used (Werling et al (*39*), human brain; Newman et al (*41*), human heart; Viguerie et al (*42*), human adipose; Zhang et al (*96*), human liver).

Expression breadth, expression constraint, and sequence conservation

To calculate expression breadth in humans, we first estimated the expression level of each gene in each of the 12 tissues as its median TPM value among the samples from that tissue. For each gene, we then normalized its TPM values across tissues to its maximum TPM value, and took the average of these normalized values across tissues. To calculate expression breadth in chicken, we used the same strategy, except with RNA-seq data from nine male tissues (*37*). Rather than comparing expression breadth (or any other gene-level trait) between genes with or without sex bias in any of the 12 tissues, we performed comparisons within each of the 12 tissues separately. This avoids artificial skewing due to detection bias; for example, broadly expressed genes, by simple virtue of their broad expression, could be more likely to be detected as sex-biased in at least one of the 12 tissues. To estimate evolutionary constraint on gene expression in mammals, we used genome-wide percentiles of evolutionary constraint from Chen et al (*47*). We measured sequence conservation by calculating the mean phyloP score for all coding bases of the longest annotated transcript of each gene.

Transcriptome-wide association study (TWAS) data

TWAS uses an eQTL study as a reference panel to impute the relative expression of a given gene, based on multiple SNPs, for individuals assessed in the GWAS. TWAS relies exclusively on eQTLs presumed to act in cis (i.e. within a fixed window around a gene). This procedure allows for association of imputed gene expression levels with the trait of interest and yields directional expression-trait associations: genes with trait-increasing effects have a positive association (Z-score) between imputed expression and the trait, while genes with trait-decreasing effects have a negative association.

We generated TWAS Z-scores using FUSION (*54*) with default parameters. We used three sources of height GWAS summary statistics: 1) the UK Biobank (*56*) (https://data.broadinstitute.org/alkesgroup/UKBB/body_HEIGHTz.sumstats.gz), 2) the GIANT consortium (*57*) (https://portals.broadinstitute.org/collaboration/giant/images/0/01/GIANT_HEIGHT_Wood_et_al_2014_publicrelease_HapMapCeuFreq.txt.gz), or 3) a meta-analysis of the two studies (*48*) (https://portals.broadinstitute.org/collaboration/giant/images/6/63/Meta-analysis_Wood_et_al%2BUKBiobank_2018.txt.gz)

For eQTL data, we used preprocessed reference panels for 48 tissues from the GTEx Consortium (v7) (*35*) downloaded from: http://gusevlab.org/projects/fusion/. For all downstream analyses, we only used Z-scores from TWAS models that were significantly predictive of expression levels, as determined by model cross-validation (Benjamini-Hochberg FDR 5%). We combined TWAS Z-scores for the same gene across tissue reference panels under a fixed-effects model,

summing all Z-scores for a gene and dividing by the square root of the number of Z-scores for that gene.

Estimating the contribution of conserved sex bias to sex differences in mean height

For each of 560 gene-tissue pairs, we have a direction of conserved sex bias (male- or female-biased) as well as a TWAS Z-score (positive means increased expression is height-increasing, negative means that increased expression is height-decreasing). In the first approach, for each gene, we used the SNP that is the best eQTL (in the same tissue as sex bias) as a proxy. We assume that all of this SNP's per-allele effect on height is mediated through cis effects on gene expression. While this assumption likely does not hold for all SNPs, we found the magnitude of a gene's sex bias to be approximately two-fold greater than the per-allele effect size of the best eQTL (fig. S5), meaning that even if only ~50% of a SNP's per-allele effect on height were mediated through cis-effects on gene expression, using the SNP as a proxy for sex bias of a gene is still reasonable. Next, we signed the height effect of the SNP based on the agreement between sex bias and the TWAS Z-score. For example, if a gene shows conserved male (female) bias and the TWAS Z-score is positive (negative), the sex bias of this gene is expected to contribute to the sex difference in height, and therefore the associated SNP effect size for this analysis should be positive. In contrast, if a gene shows conserved male (female) bias and the TWAS Z-score is negative (positive), the sex bias of this gene should reduce the sex difference in height, and therefore the associated SNP effect size should be negative. Making the common assumption of an additive contribution of each SNP to height, we sum up all such signed effect sizes to obtain an estimate of the contribution of conserved sex bias in gene expression to sex differences in height. Finally, since height effect sizes are reported in terms of sex-specific standard deviations

(6.2 cm in UK Biobank females, 6.6 cm in UK Biobank males), we multiplied the summed effect sizes by 6.4, the mean of the male and female standard deviations.

In the second approach, we computed height fold-changes directly from TWAS Z-scores. Under the assumption that standard errors of TWAS effect sizes are proportional to GWAS sample size *N*, $\beta = \frac{Z}{\sqrt{N}}$. Here, β represents the correlation between imputed expression and height. However, the imputation of expression can only be as good as the overall cis-heritability of gene's expression levels, h^2_{cis}, which is measured in the reference eQTL panel. Assuming that inaccuracies in imputation are randomly distributed, lower heritability (closer to 0) would mean a lower true correlation between expression and height, thus the correlation between true expression and height can then be defined as $\beta_{cis\ adj} = \beta * h^2_{cis}$. This number represents the percentage change in height as a result of a 100% increase (i.e. doubling) of expression. For all of the gene-tissue pairs under consideration, the magnitude of sex bias is smaller than a 100% change – we therefore defined $\beta_{cis,sex\ adj} = \beta_{cis\ adj} * p_{sex}$, where p_{sex} is the percentage increase in either sex. $\beta_{cis,sex\ adj}$ represents the percentage change in height as a result of sex bias of a given gene-tissue pair. As in the first approach, we signed $\beta_{cis,sex\ adj}$ based on the agreement between the direction of sex bias and the direction of the TWAS Z-score for each gene-tissue pair and summed all $\beta_{cis,sex\ adj}$ to obtain an estimate of the total percentage change in height explained by conserved sex bias.

cis-eQTL effect sizes

To quantify cis-eQTL effect sizes, we relied on $\log_2$ allelic fold change (aFC) estimates, which are provided for significant eGene associations (https://storage.googleapis.com/gtex_analysis_v7/single_tissue_eqtl_data/GTEx_Analysis_v7_e

QTL.tar.gz). aFC represents the expected $\log_2$ fold-change in expression between individuals homozygous for either the reference or alternative allele (i.e. 0 vs 2 copies of the alternative allele) (*97*); however, in this study we focus on the per-allele effects of the best eQTL on height as reported in GWAS. Therefore, we converted aFC estimates to a per-allele estimate using the formula $aFC_{het} = log_2(\frac{2^{aFC}+1}{2})$, where aFC is the original estimate and aFC_{het} is the new estimate which represents the expected $\log_2$ fold-change in expression between individuals homozygous for the reference allele and heterozygous for the reference and alternative alleles.

Motif analysis

We identified motifs enriched in the promoters (± 1 kb around the most distal transcription start site as annotated in human GENCODE v26, or in each of our improved non-human mammalian transcriptomes) of genes with lineage-specific sex bias using a two-step procedure adapted from a recent study of epigenetic poising in the mammalian germline (*98*). In the first step, we used DREME (*79*) with default settings to identify motifs enriched in the promoters (± 1 kb around the most distal transcription start site) of each set of lineage-specific sex-biased genes within each tissue. For any given type of lineage-specific bias, we only analyzed tissues with FDR < 0.30 as assessed by permutation. In the second step, we used AME (*80*) to scan 100 random, equally sized sets of orthologous promoters for enrichment of the motifs detected in the first step. The fraction of random promoter sets showing motif enrichment with a lower p-value than that of the motif in the true promoter sets (which was re-estimated using AME) constituted a raw p-value. This second step ensures that the DREME motif enrichment is specific to the genes in question and not the result of an overall enrichment of the motif in the species or lineage in question. P-values from all tissues for a given type of lineage-specific sex bias (e.g., primate loss

or rodent gain) were then adjusted by the Benjamini-Hochberg method. We matched motifs with FDR < 0.10 to binding sites for known transcription factors from the JASPAR (*99*) Core vertebrates database using TOMTOM (*100*) with parameters –thresh 10 -evalue -dist ed.

We devised a simple metric to estimate the fraction of lineage-specific sex biases which are accounted for by gains or losses of motifs for sex-biased TFs. For each of the 83 instances where the gained or lost motif corresponded to a sex-biased TF in the same tissue (e.g., matches for PKNOX1 motif in genes with a primate loss of sex bias in muscle), we computed the difference between the number of sex-biased orthologs with a motif match (the "observed" number) and the number expected in the promoters of non-sex-biased orthologs, as calculated by DREME in the initial discovery step. This calculation was done at the level of orthologs in individual species (i.e., for genes with a primate gain of sex bias, human and cyno orthologs are considered independently); to avoid such double counting, we divided this number by two if the sex bias gain/loss in that tissue involved two species in the phylogeny in this study. We then multiplied this calculated excess by the estimated true positive rate (1 - FDR) for that specific lineage/tissue combination. These estimates for each of the 83 instances, provided in Table S9, were then summed up to obtain the total estimated number of sex-biased gene-tissue pairs which could be accounted for by motifs for sex-biased TFs.

Validation of TF binding with ChIP-seq data

For sex-biased TFs with publicly available data, ChIP-seq peaks (.bed files) were downloaded from the source indicated in Table S9. Each set of TF peaks was then intersected with the set of all promoters (± 1 kb around the most distal transcription start site) for all genes using bedtools (*101*); a gene was classified as TF-bound if it contained at least one ChIP-seq peak. Motif-

containing genes (human or mouse, as all analyzed ChIP-seq data were from these two species) were identified by running FIMO (*102*) on the same promoter sequences using the motif discovered in the above-described DREME step. The TF-bound fraction of motif-containing, sex-biased genes of the relevant evolutionary class (i.e. rodent gain in muscle) was compared to the TF-bound fraction of all expressed one-to-one orthologs without a motif by Fisher's exact test.

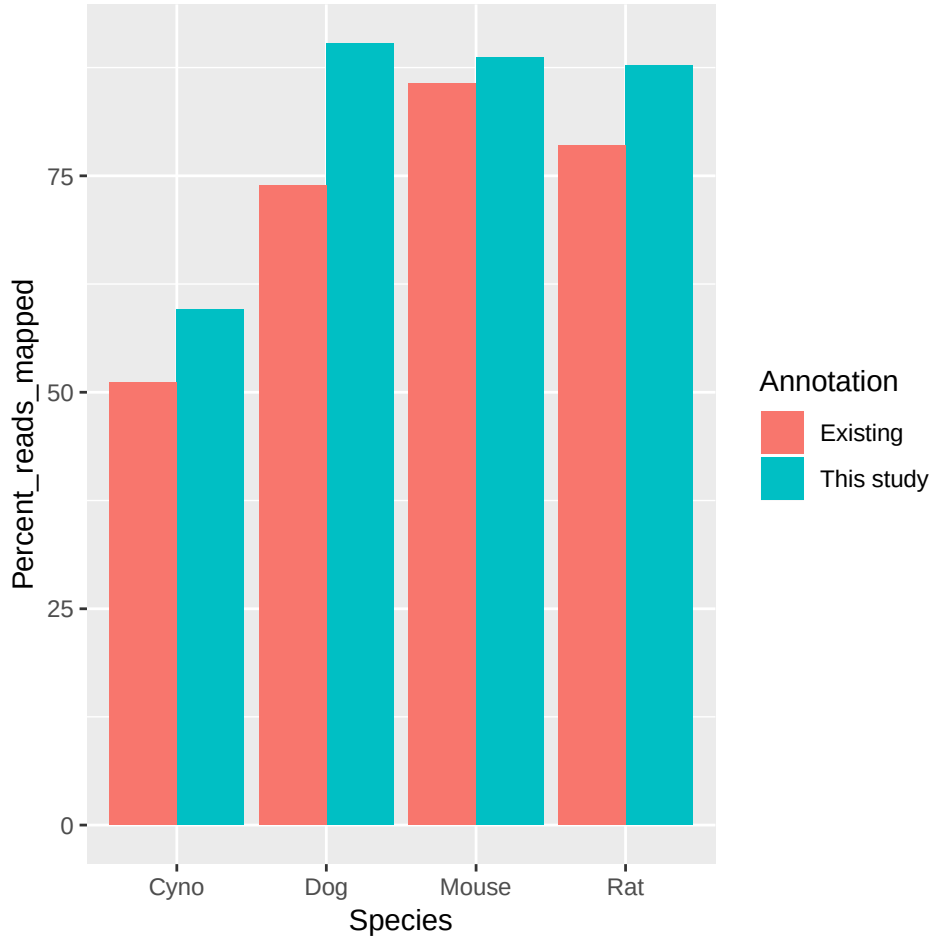

Fig. S1: Comparison of read mapping rates between existing transcriptome annotations and those generated as part of this study. For each species, RNA-seq reads from an independent study (cyno, M5 Spleen from https://doi.org/10.6084/m9.figshare.4697539.v2; dog, SRR388736; mouse, SRR594408; rat, SRR594435) were pseudomapped to either Ensembl 91 transcript annotations or annotations from this study using salmon.

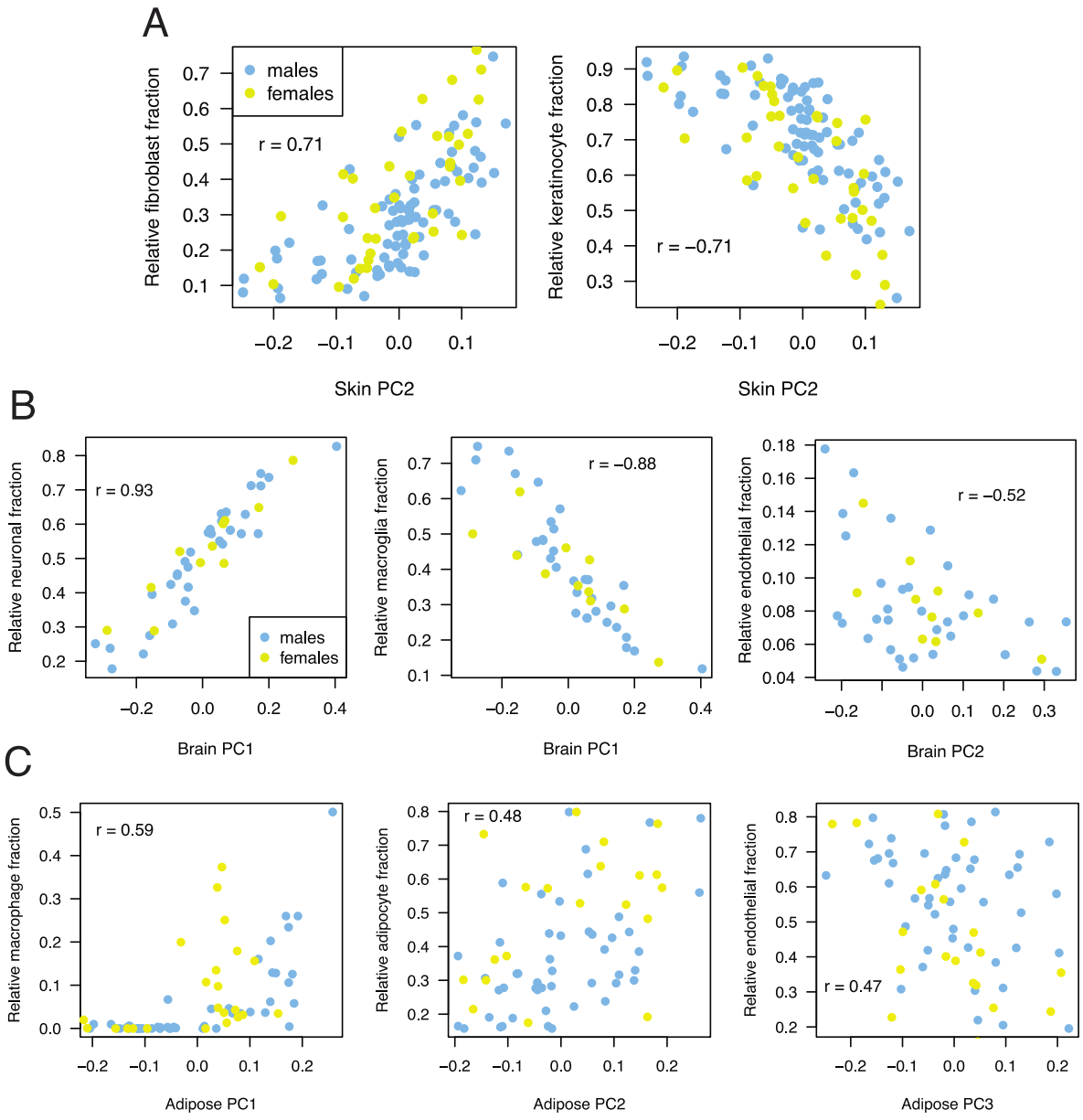

Fig. S2: Correlation between sample loadings on top principal components with estimated cell-type fractions. For each tissue (A, skin; B, brain; C, adipose), sample loadings (x-axis) for the top principal components were estimated as described in Methods. The y-axis represents the proportion of the indicated cell-type estimated as estimated by CIBERSORT (see Methods). Each plot is annotated with a Pearson correlation coefficient.

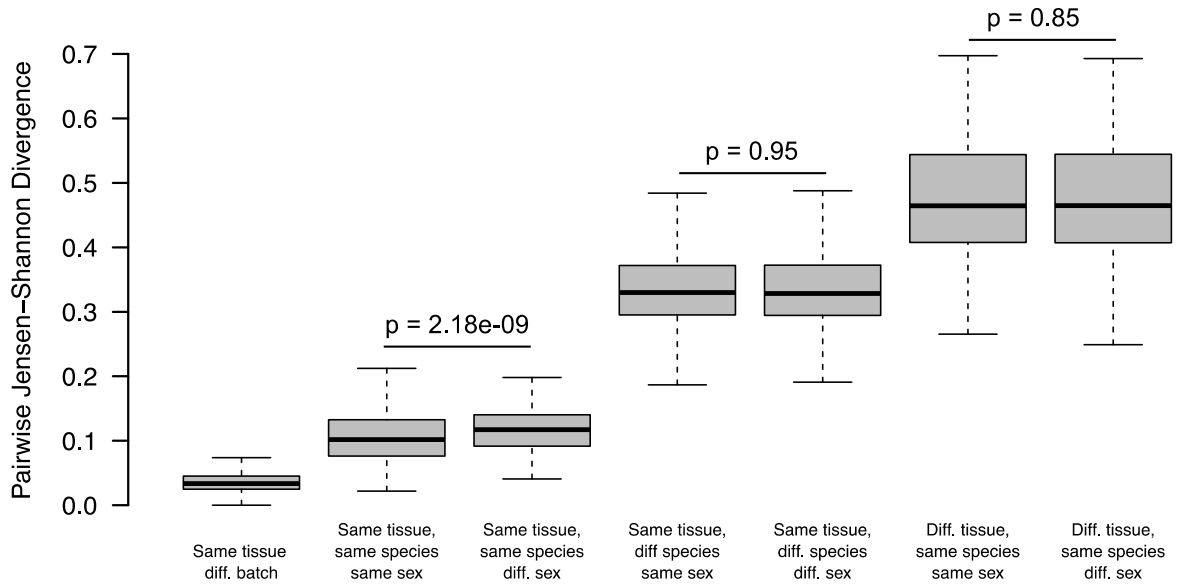

Fig. S3: Sources of biological and technical variation. Each boxplot represents JSD values for all pairs of samples meeting the described criteria below. The left-most boxplot represents technical variation due to library preparation and sequencing, while the other boxplots represent biological sources of variation. Indicated p-values from two-sided Wilcoxon rank-sum test comparing distances within or between sex for samples in the same/different tissue or species. P-values for all other comparisons were < 2.2e-16 by two-sided Wilcoxon rank-sum test.

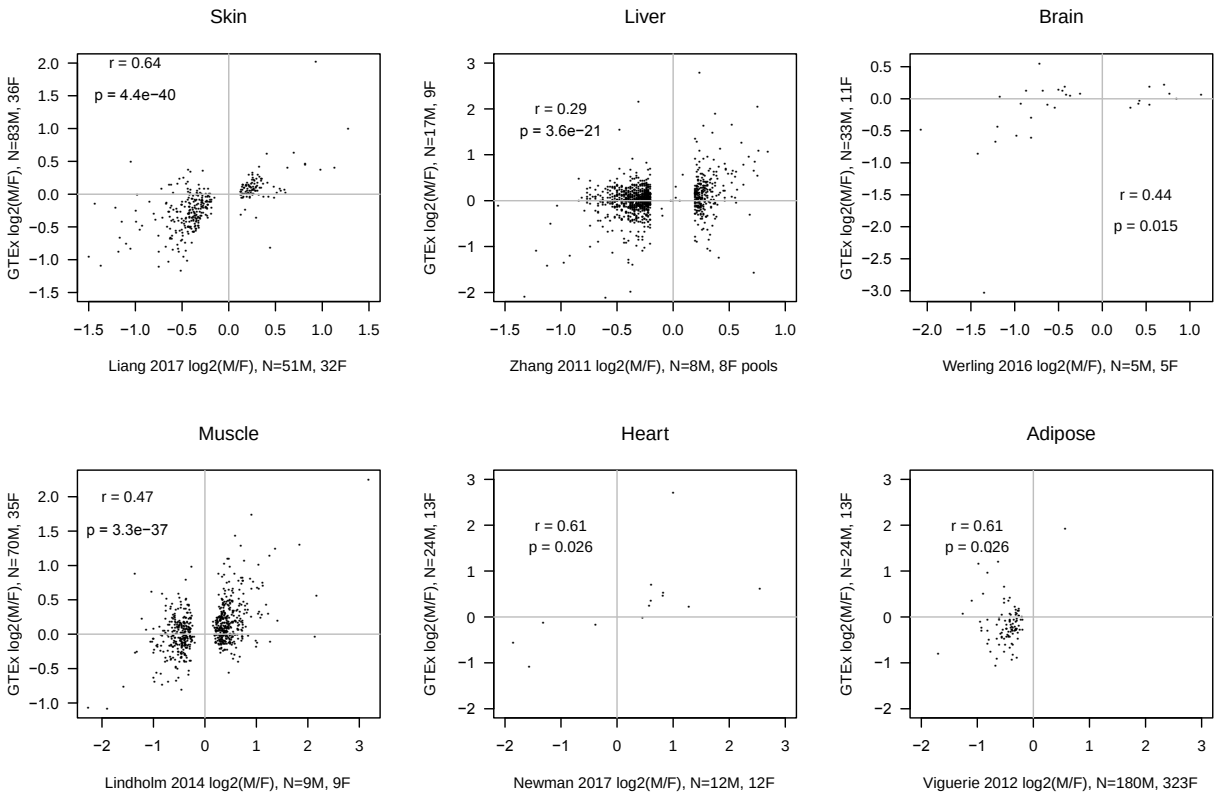

Fig. S4: Correlation between published estimates of sex bias and estimates of sex bias in this study (human). For each tissue, significantly sex-biased genes from published studies were defined as described in Methods. The x-axis represents sex bias from the independent study, and the y-axis represents sex bias from our re-analysis of GTEx. Each plot is annotated with a Pearson correlation coefficient.

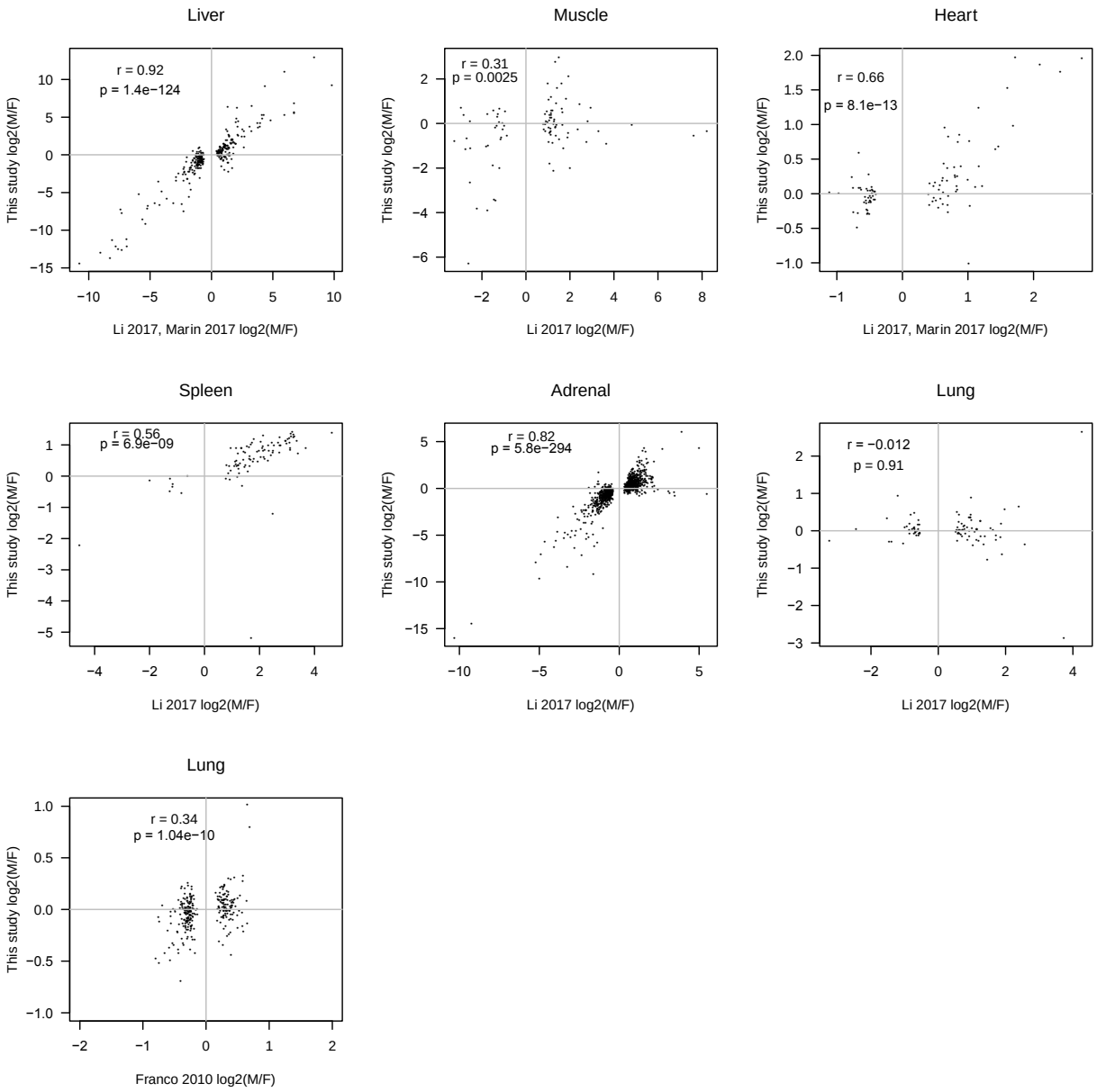

Fig. S5: Correlation between published estimates of sex bias and estimates of sex bias in this study (mouse). For each tissue, significantly sex-biased genes from published studies were defined as described in Methods. The x-axis represents sex bias from the independent study, and the y-axis represents sex bias from data newly generated as part of this study. Note that for lung, estimates from Li et al. (2017) do not replicate, but estimates from Franco et al. (2010) do replicate. Each plot is annotated with a Pearson correlation coefficient.

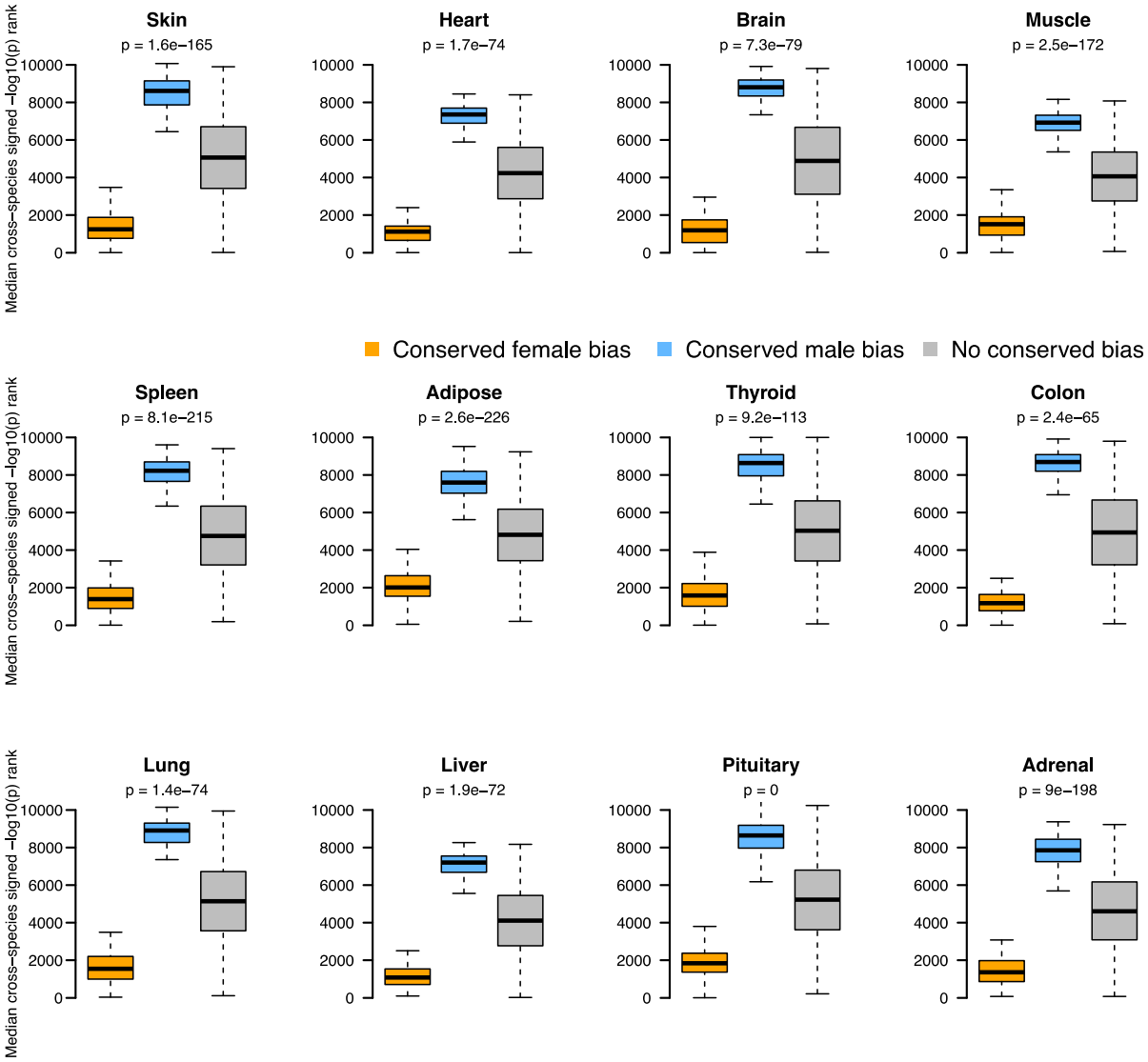

Fig. S6: Non-parametric validation of conserved sex bias as detected using a linear mixed model approach. Rank-based statistic for conserved sex bias (see Materials and Methods for details on calculation) plotted for genes in each tissue identified by the linear mixed model approach as showing conserved female (orange) or male (blue) bias, or no bias (grey). P-values determined by Kruskal-Wallis test.

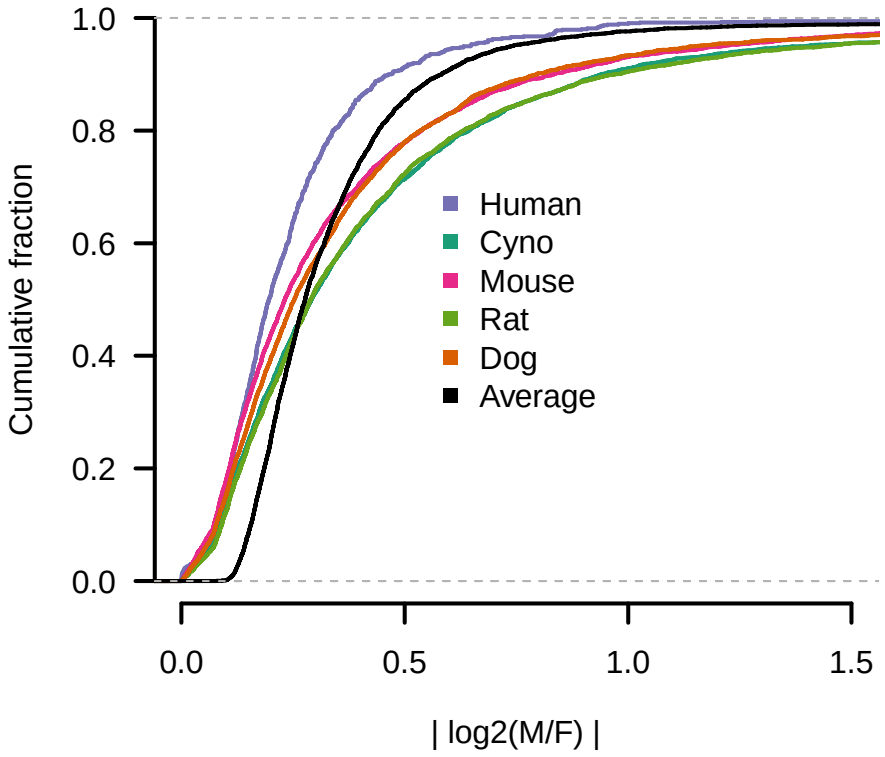

Fig. S7: Magnitude of male/female difference in expression of genes with conserved sex bias. Cumulative distribution plots of the magnitude of sex bias (estimated by simple linear regression in each species), for all gene-tissue pairs with a conserved sex bias.

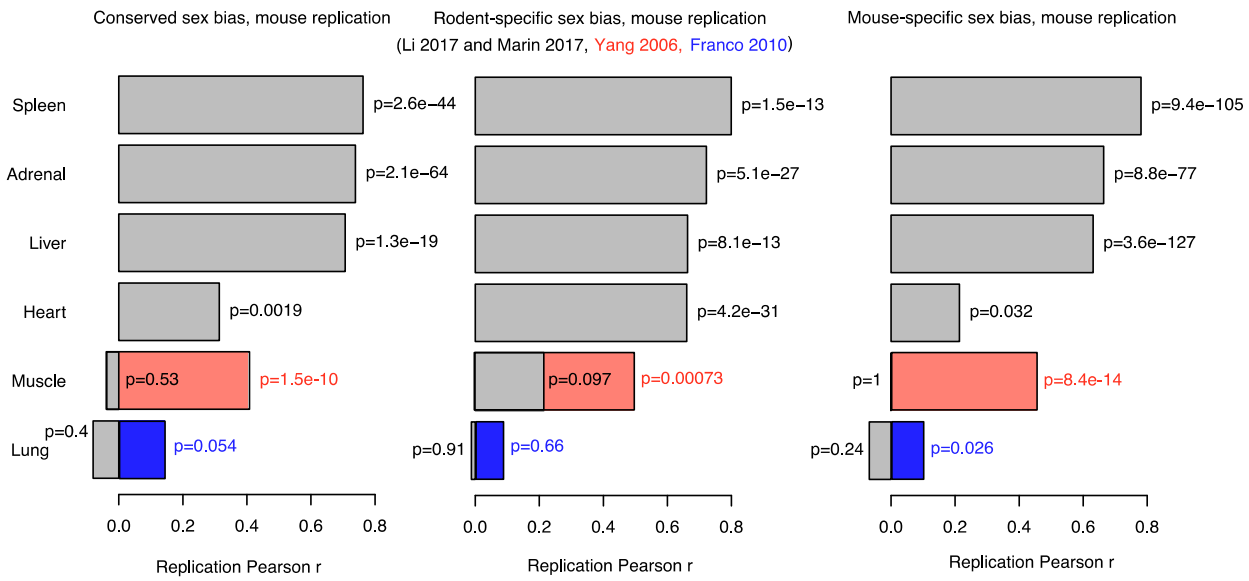

Fig. S8: Correlations between estimates of sex bias for evolutionary classes of sex-biased genes from this study with estimates from independent studies (mouse). For conserved (left), rodent-specific (middle), or mouse-specific (right) sex biases defined as described in Materials and Methods, the correlation between sex bias estimates from our study and independent studies is shown.

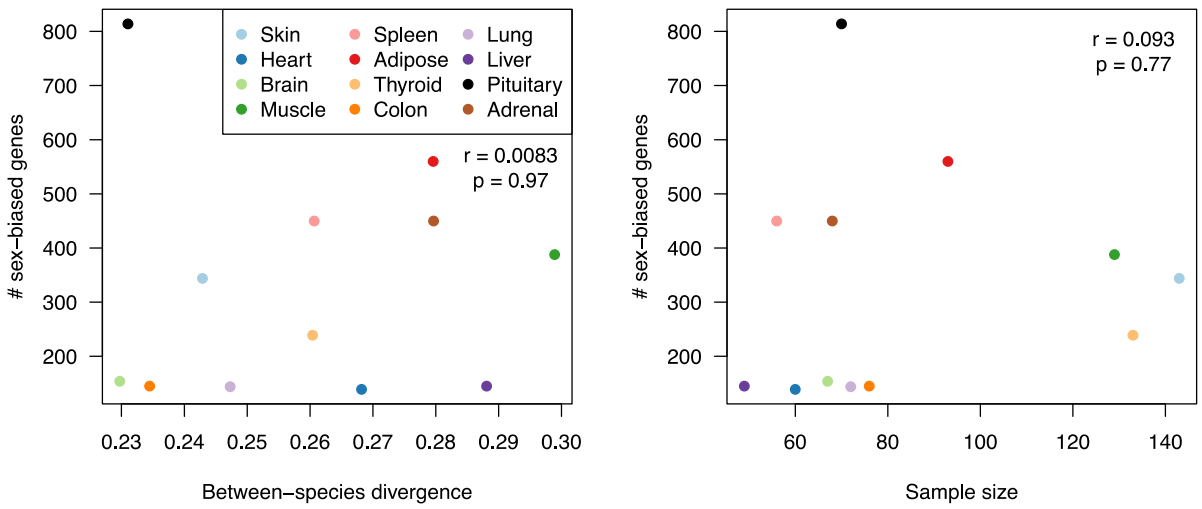

Fig. S9: No correlation between extent of conserved sex bias and sample size or expression divergence of tissues. Between-species divergence for each tissue was calculated as the median JSD for all pairs of samples from that tissue but from different species.

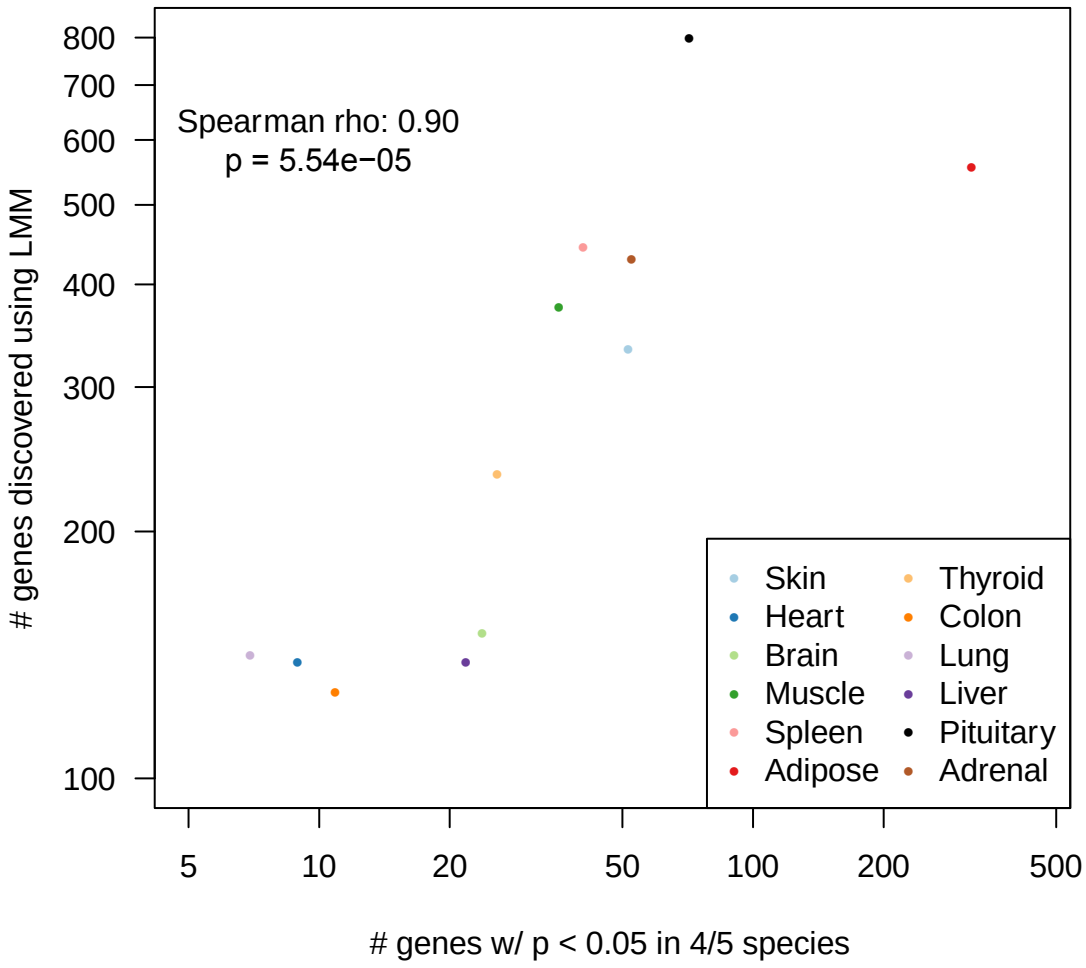

Fig. S10: Comparison of by-tissue numbers of genes with conserved sex bias using either a naïve approach (x-axis) or a linear mixed model approach (y-axis).

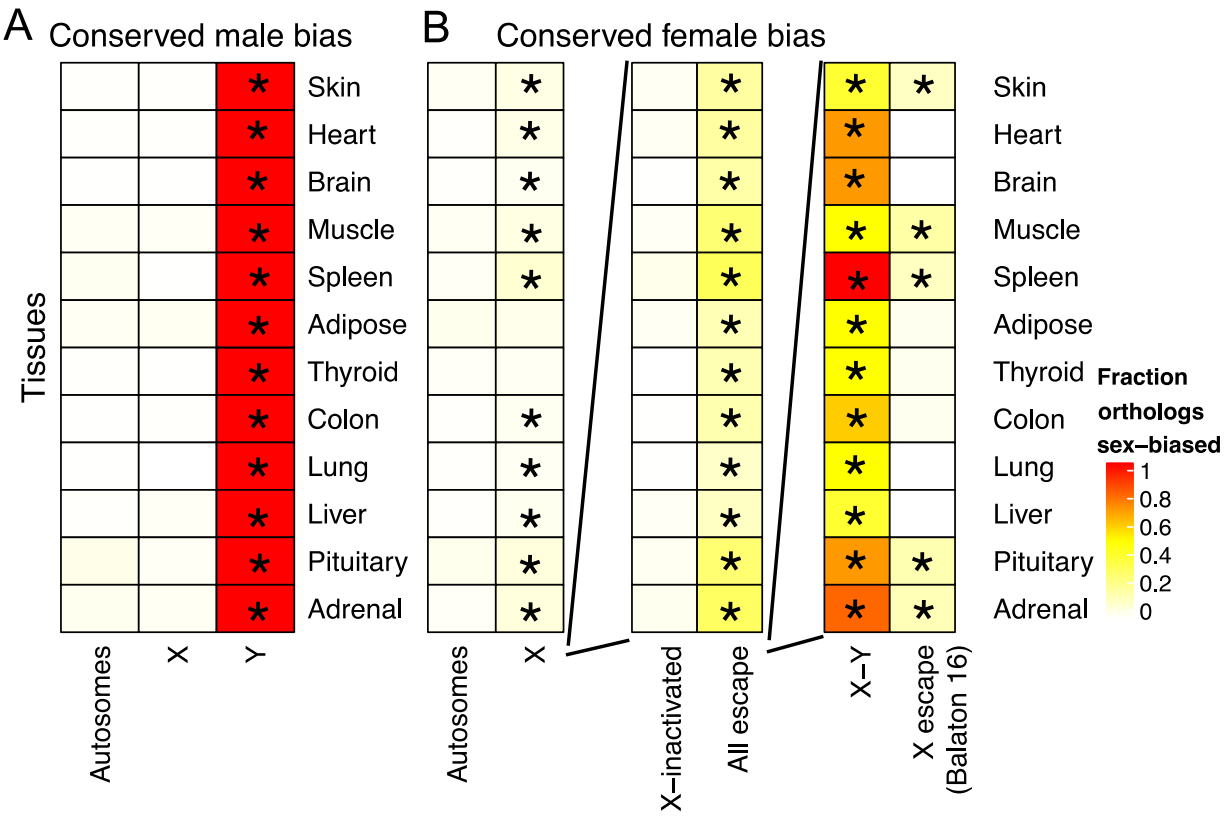

Fig. S11: Enrichment of genes with conserved female or male bias with respect to autosomes, sex chromosomes, and classes of sex-linked genes. Colors represent the fraction of analyzed one-to-one orthologs on the indicated chromosome(s) with conserved male (A) or female (B) bias. For female bias, all X-linked genes (left) are further subdivided into those previously annotated as escaping or subject to X-inactivation in females by a recent meta-analysis of three studies (middle). X escape genes are further subdivided into those with or without a surviving Y-linked homolog (right). *, Benjamini-Hochberg-adjusted p-value < 0.05, two-sided Fisher's exact test comparing to autosomes.

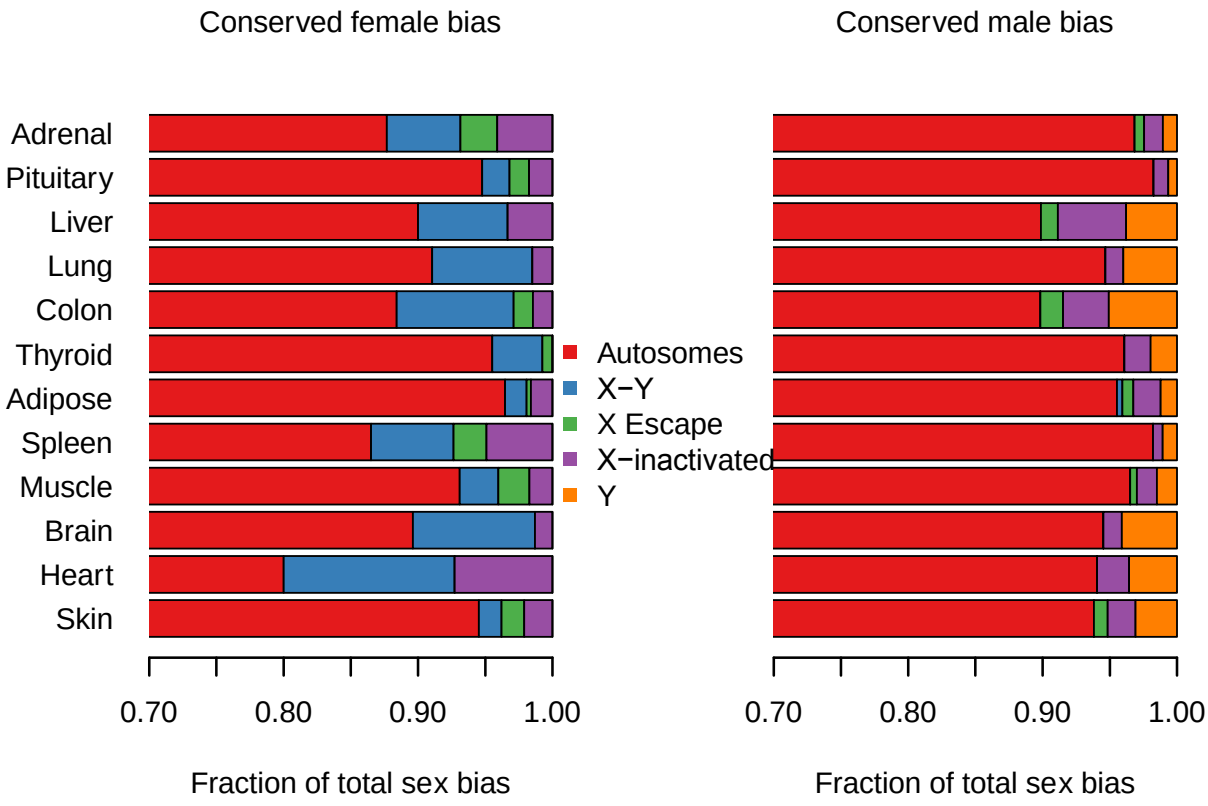

Fig. S12: Fractions of genes with conserved female (left) or male (right) bias on autosomes, sex chromosomes, or classes of X-linked genes.

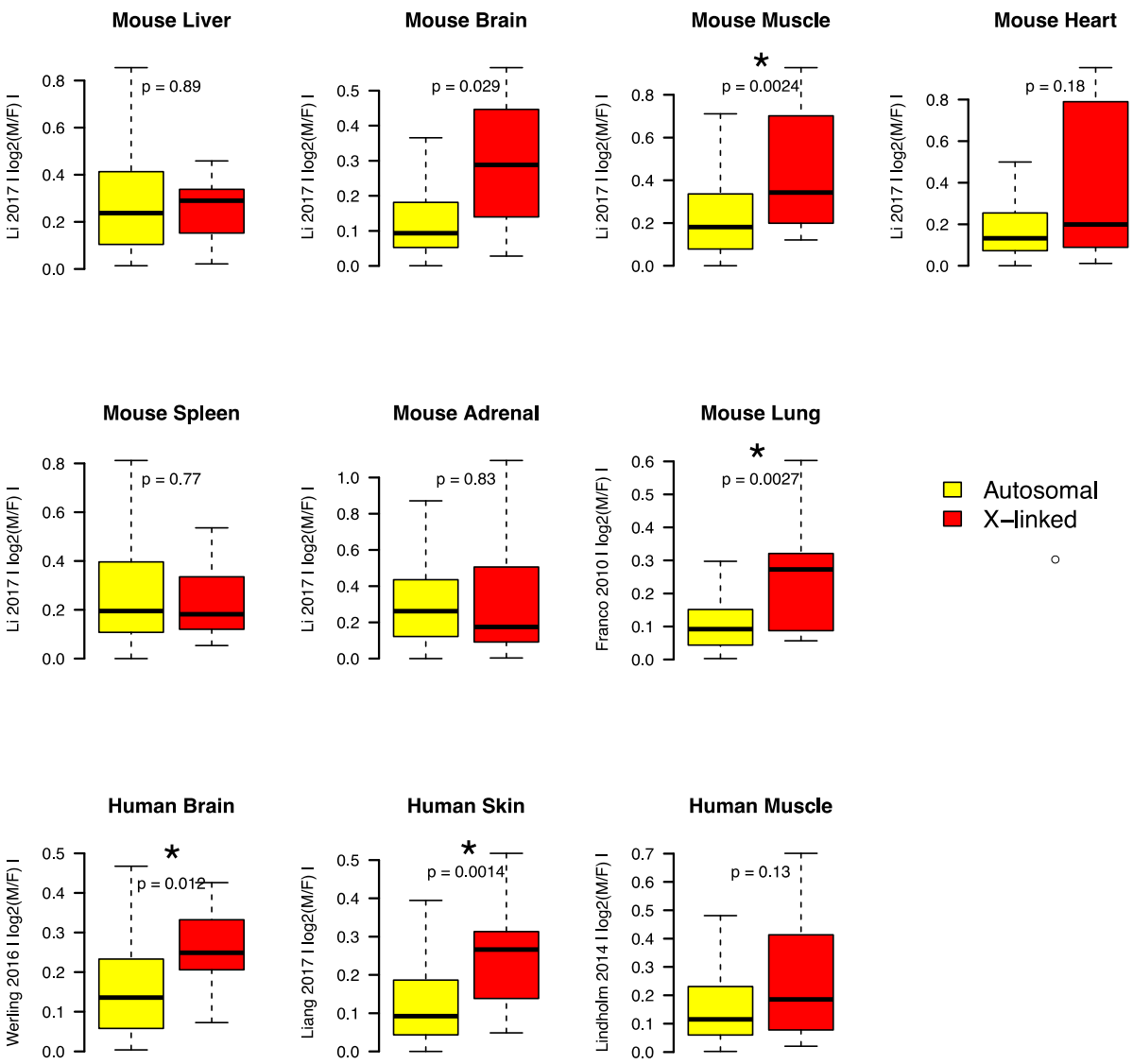

Fig. S13: Comparison of fold-changes between X-linked (yellow) and autosomal (red) genes in independent human and mouse datasets. *, Benjamini-Hochberg-adjusted p-value (two-sided Wilcoxon rank-sum test) < 0.05.

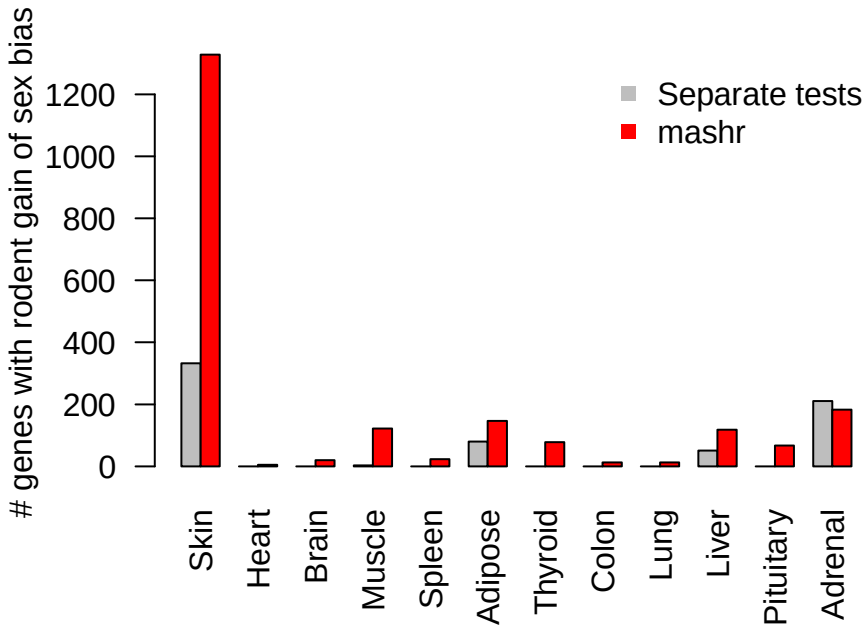

Fig. S14: Increased detection of rodent gains of sex bias using mashr. Number of genes detected as having a rodent-specific sex bias (male or female) in each tissue when using standard separate tests for each species (grey, limma/voom FDR < 0.1 and same direction of bias in mouse and rat only) versus when using mashr (red) as described in Methods.

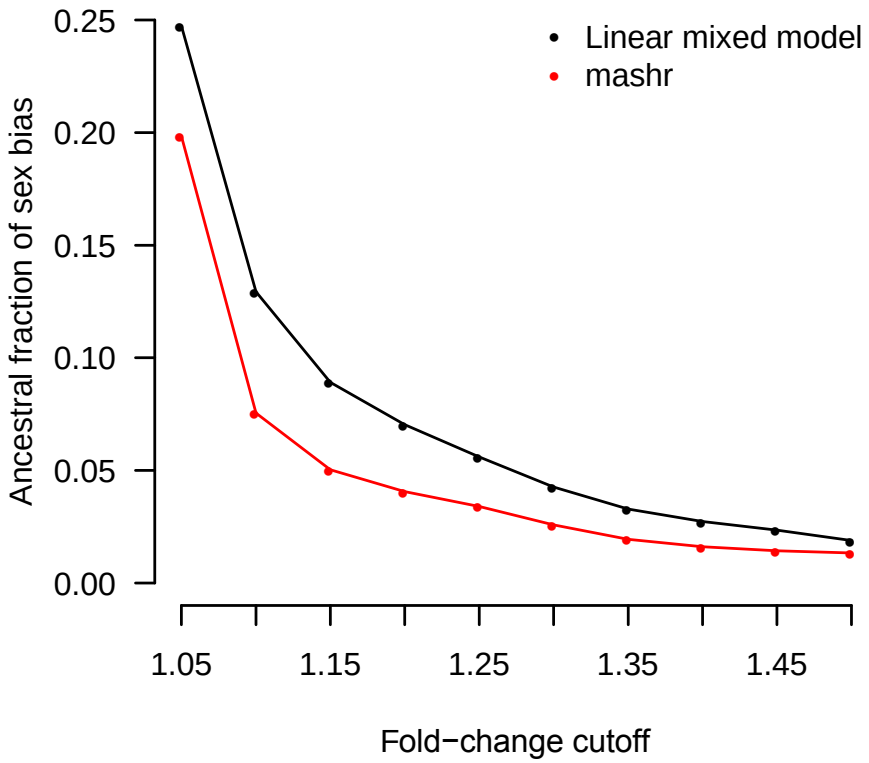

Fig. S15: Fraction of total sex bias found to be ancestral when applying a range of fold-change cutoffs to define both ancestral and acquired sex bias, using the linear mixed model approach (black) or mashr (red). The ancestral fraction of sex bias at each fold-change cutoff was calculated as in Fig. 3B, using the empirically calculated FDRs to estimate the number of true-positive gene-tissue pairs with ancestral or acquired sex bias.

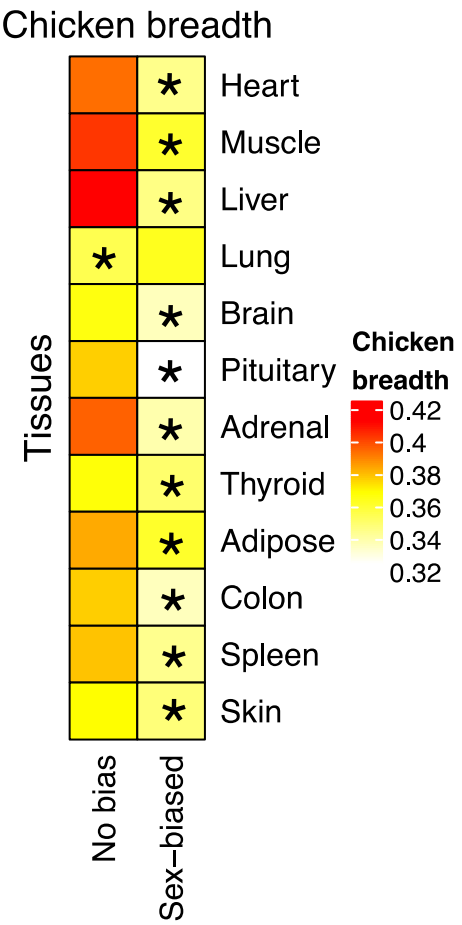

Fig. S16: Differences in chicken expression breadth between genes with or without sex-biased gene expression. Chicken expression breadth was calculated using RNA-seq data from nine male tissues from Merkin et al. (2012). In the heatmap, the group median of expression breadth is plotted, and asterisks indicate a Benjamini-Hochberg adjusted p-value < 0.05 for a two-sided Wilcoxon rank-sum test, placed on the group ("No bias" or "Sex-biased") with the lower median expression breadth.

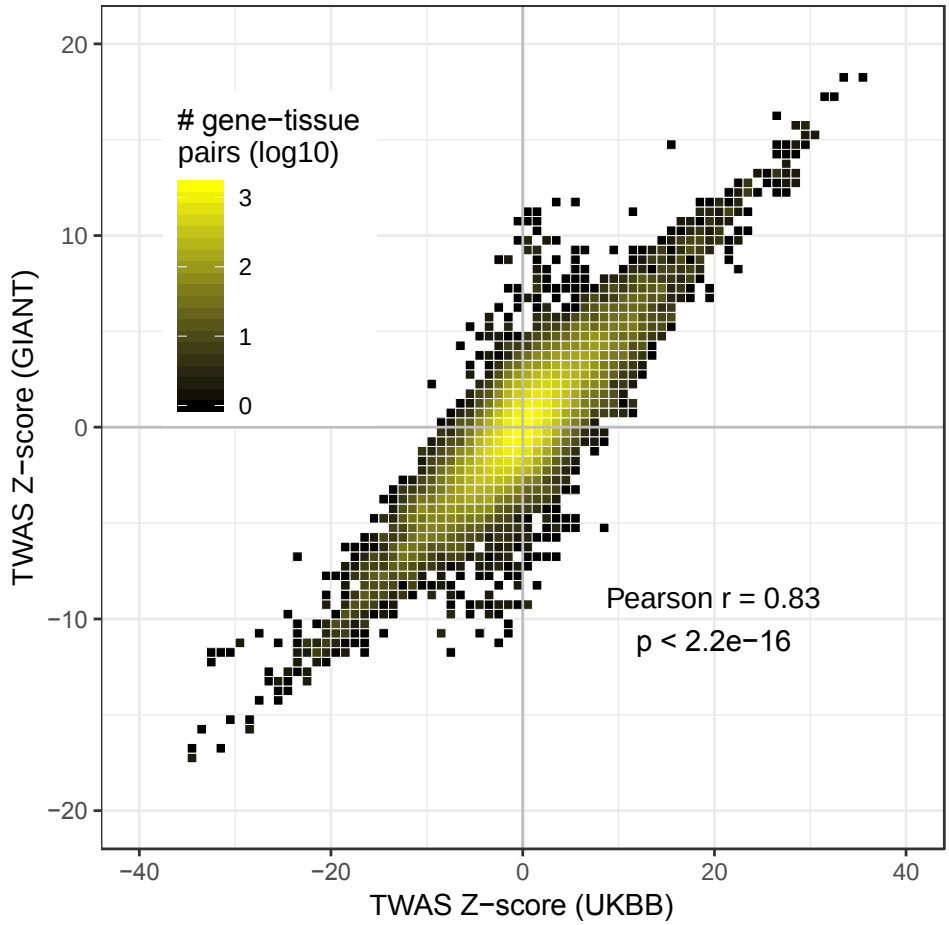

Fig. S17: Correlation of TWAS Z-scores using either UK Biobank (x-axis) or GIANT height (y-axis) GWAS. Each point represents the TWAS Z-score for a gene in a single eQTL reference panel (one of 48 GTEx tissues).

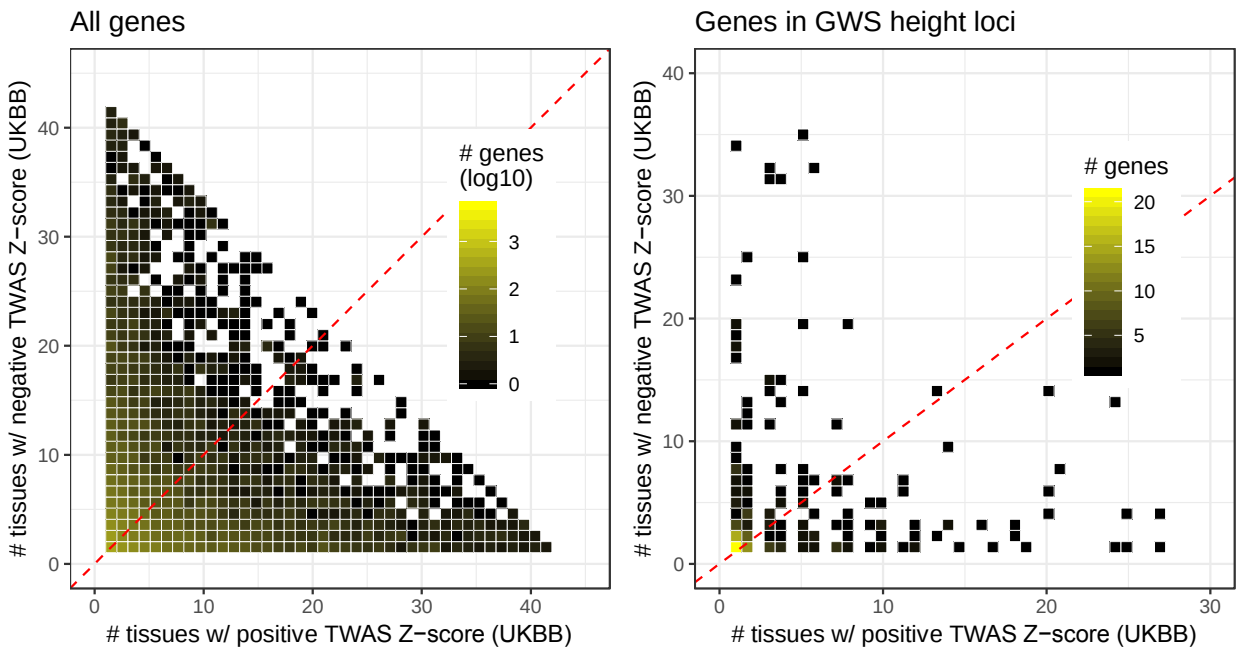

Fig. S18. Cross-tissue agreement of genic TWAS Z-scores. For each gene (left, all genes; right, all genome-wide significant height genes from the GWAS catalog), the number of tissues with positive (x-axis) or negative (y-axis) Z-scores is plotted.

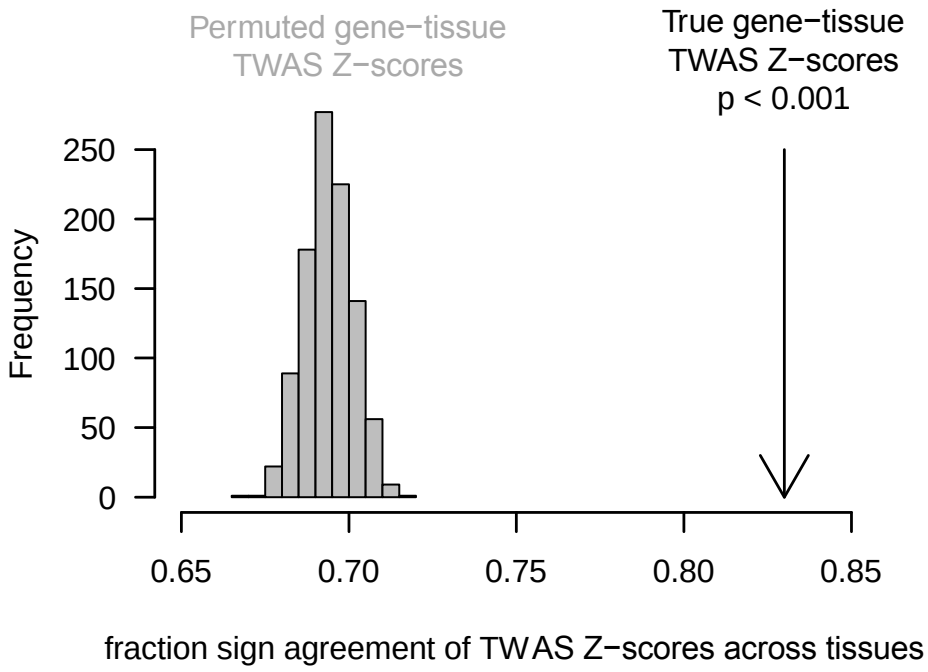

Fig. S19: Greater cross-tissue agreement of genic TWAS Z-scores than expected by chance. Fraction of tissues which agree in sign with respect to TWAS Z-scores, averaged across all genes (Fig. S18). The average fraction for true TWAS Z-scores is in black, and the fractions obtained when permuting the TWAS Z-scores among gene-tissue pairs are shown in grey.

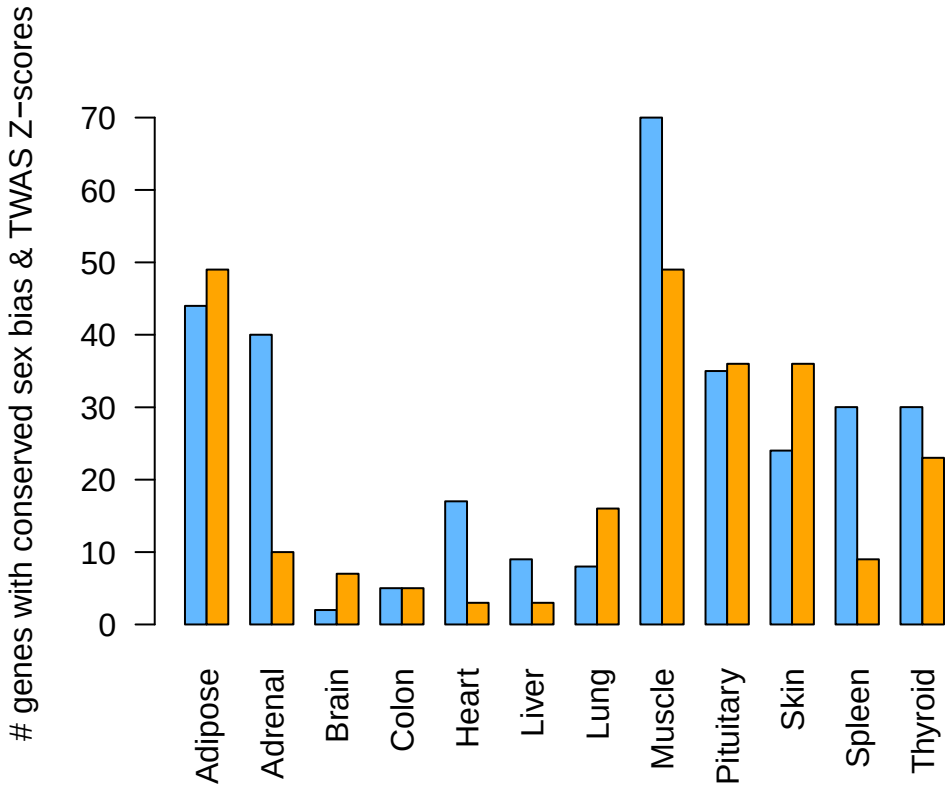

Fig. S20: Representation of conserved sex bias and TWAS Z-scores among 12 tissues. For each tissue, the number of genes with both conserved sex bias (blue, male bias; orange, female bias) and significantly predictive TWAS Z-scores is shown.

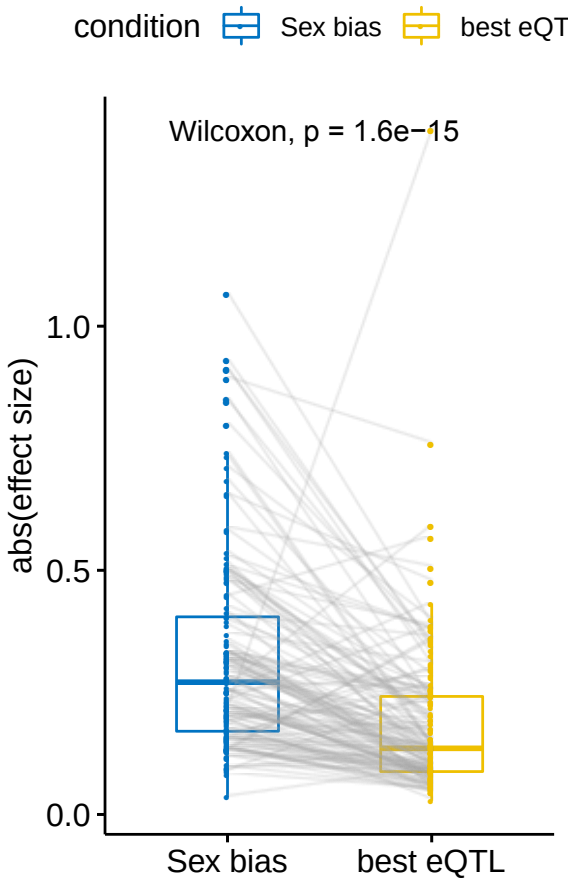

Fig. S21: Comparison of effect sizes for conserved sex bias and eQTLs. For sex bias, the effect size (y-axis) is the $\log_2$(M/F) expression ratio of the gene in the tissue in which it is sex-biased. For the best eQTL, we used the $\log_2$ allelic fold-change (aFC) in the same tissue as sex bias, when it was available, scaled to a per-allele estimate (see Materials and Methods).

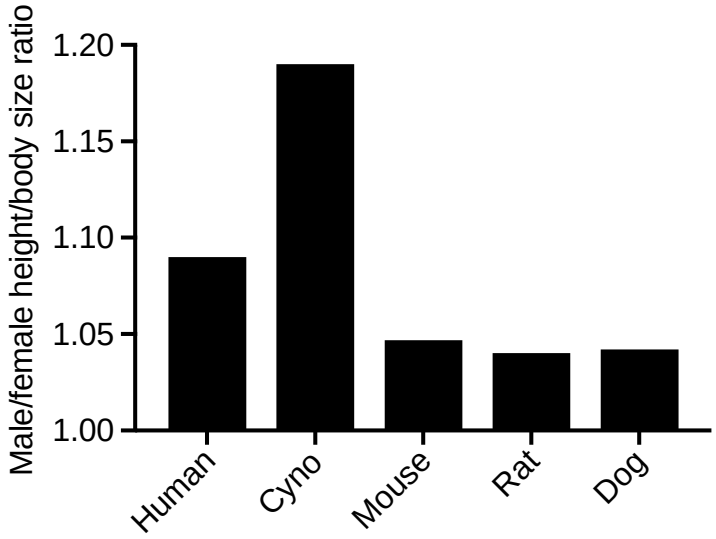

Fig. S22: Published estimates of sexual size dimorphism in the five species. Estimates from human (*53*), cyno (*103*), and dog (*104*) represent male/female standing height ratios, while mouse (*105*) and rat (*106*) represent male/female length ratios (nose to anus/base of tail).

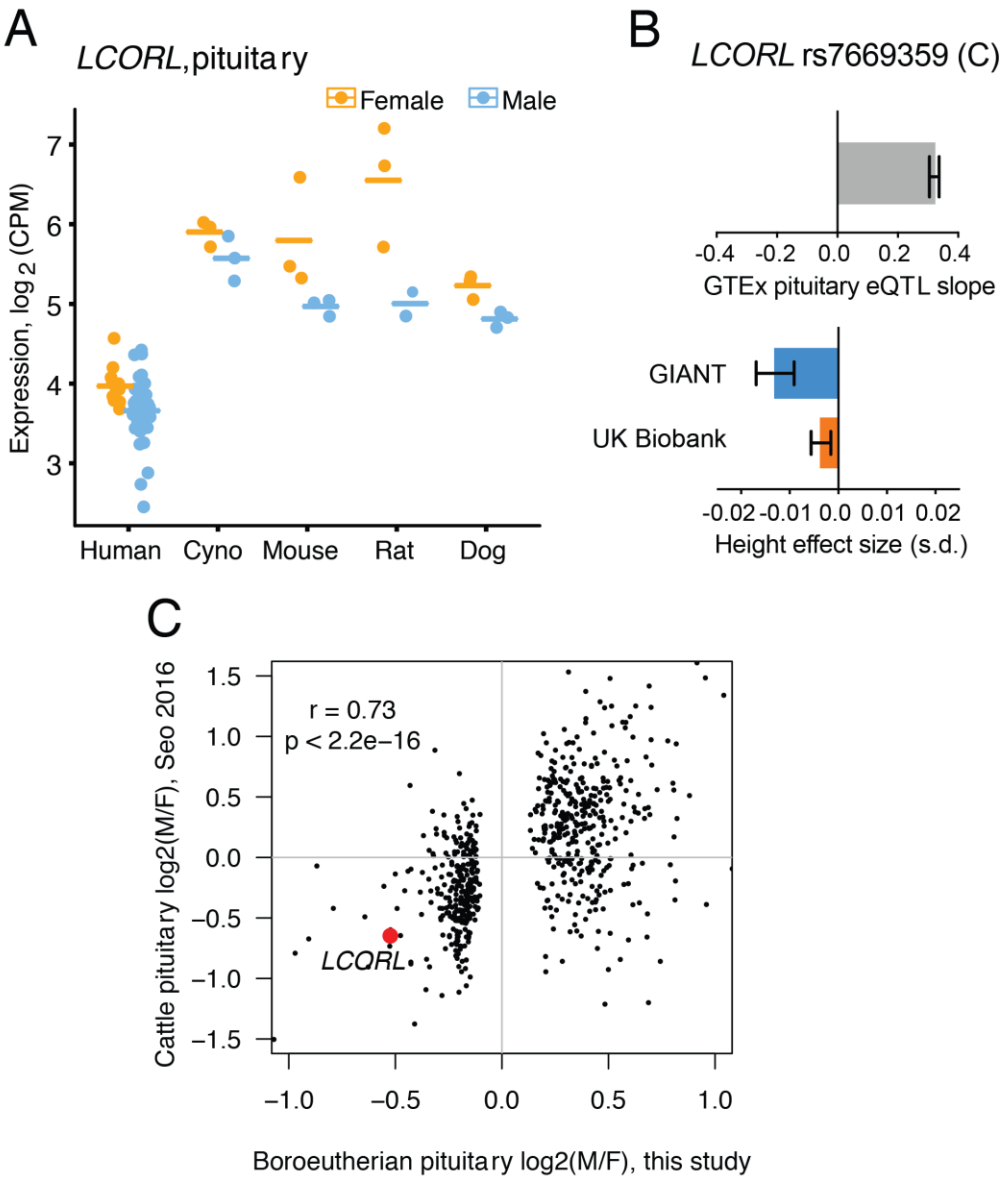

Fig. S23: Conserved sex bias and expression-height associations for *LCORL*. (A) Conserved female bias of *LCORL*, a transcription factor genetically associated with height, in the pituitary gland. (B) For a SNP at the *LCORL* locus, the effects on *LCORL* expression in the pituitary gland (top) and height (bottom) are plotted as mean +/- standard error. (C) For every gene with conserved sex bias in the pituitary, the average sex bias across the five species (human, cyno, mouse, rat, and dog, x-axis) is compared to sex bias in the cattle pituitary (y-axis).

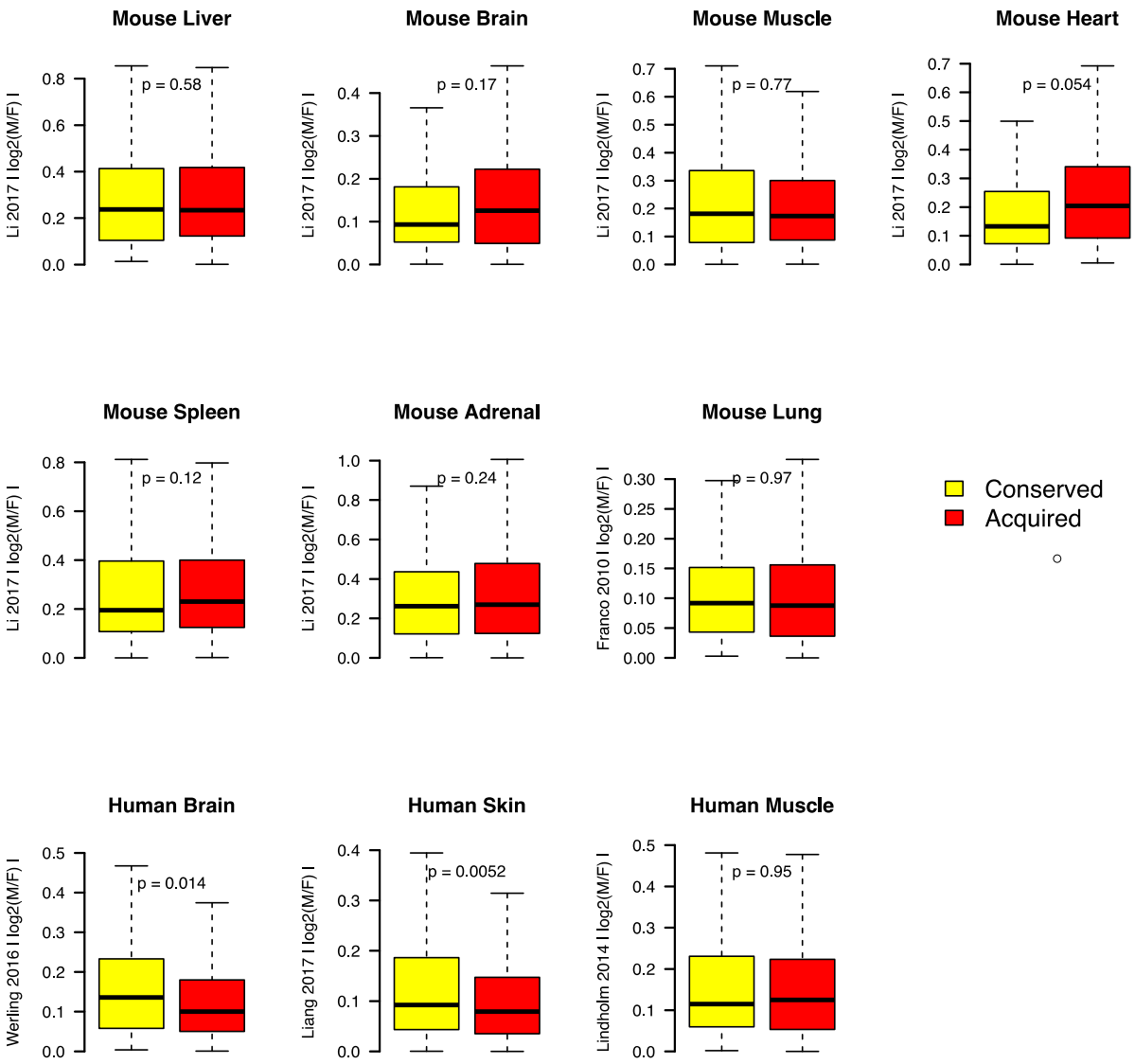

Fig. S24: Comparison of fold-changes between genes with conserved (yellow) and acquired (red) genes in independent human and mouse datasets. Unadjusted p-values (two-sided Wilcoxon rank-sum test) are provided, but note that no comparisons were significant after Benjamini-Hochberg adjustment for multiple testing.

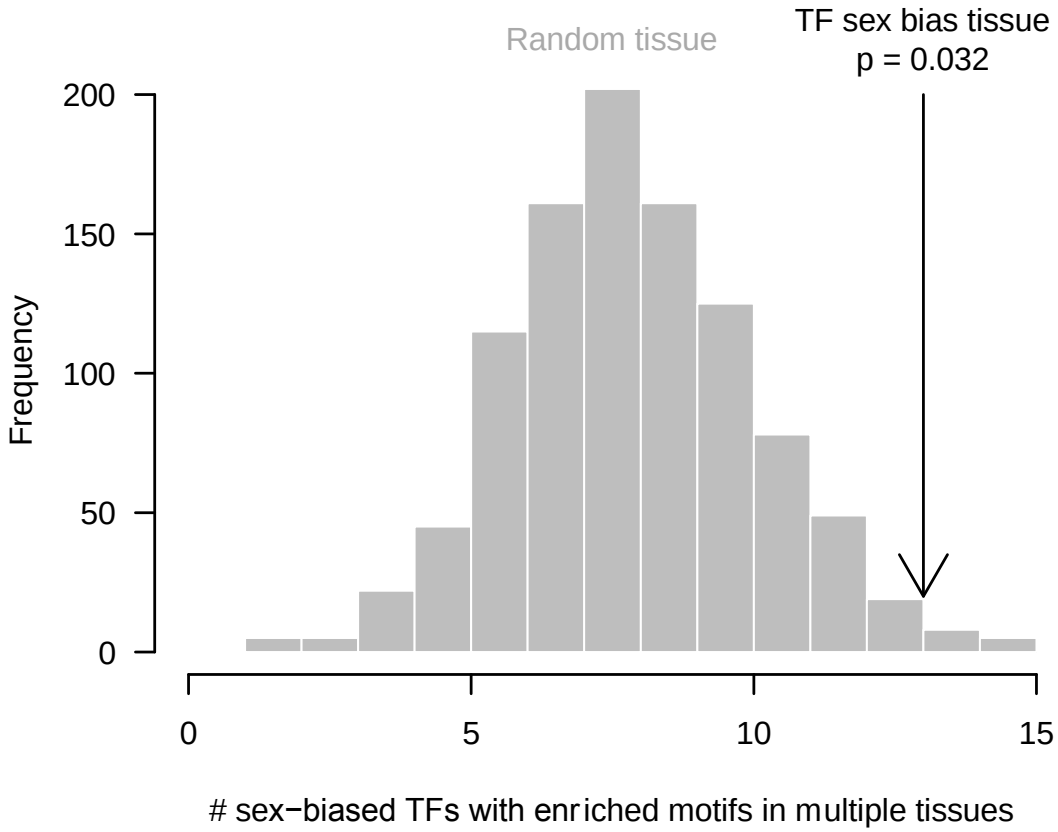

Fig. S25: Number of TFs with enriched motifs in multiple tissues expected by randomly choosing a tissue for TF sex bias, compared to the true such number of TFs.

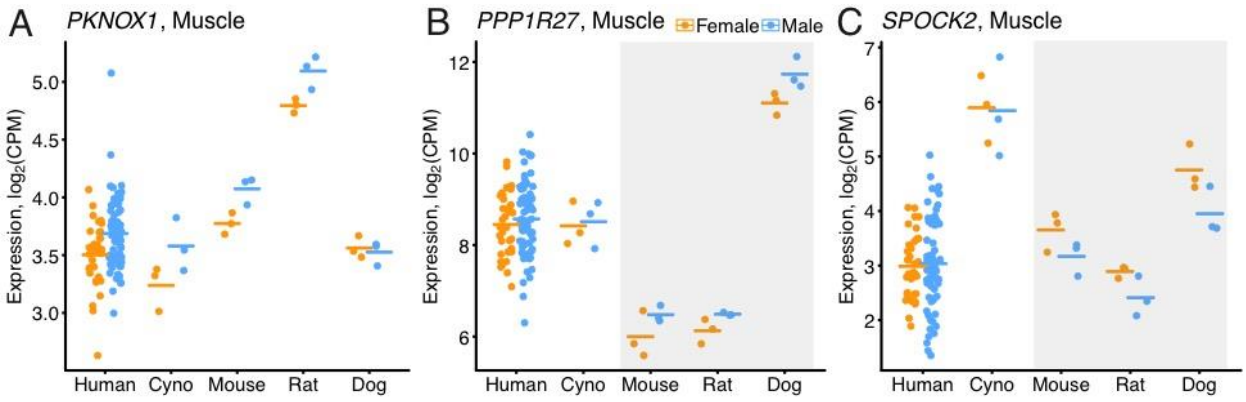

Fig. S26: Conserved sex bias of PKNOX1 (A) and representative PKNOX1 motif-containing genes with primate loss of sex bias (B, C).

Table S1.
Metadata for non-human RNA-seq libraries.

<Excel file >

Table S2.
Metadata for analyzed human GTEx RNA-seq libraries.

<Excel file >

Tissue	Male	Female
Adipose	23	48
Adrenal	20	25
Brain	11	33
Colon	25	28
Heart	13	24
Liver	9	17
Lung	11	38
Muscle	35	70
Pituitary	12	36
Skin	36	83
Spleen	16	17
Thyroid	33	77

Table S3: Number of human GTEx samples analyzed by sex and tissue.

Table S4.
Information on tissue-specific sex-biased expression, orthology assignment, and additional gene-level attributes as well as empirically estimated false discovery rates for each evolutionary class of sex bias in each tissue.

<Excel file >

Table S5.
Height TWAS Z-scores and sex bias assignments for all gene-tissue pairs.

<attached .txt file>

Table S6.

Within-tissue Gene Ontology enrichments for genes with either conserved or acquired sex bias relative to those without. Output from PANTHER statistical overrepresentation test with genes with conserved or acquired male or female bias as foreground and all genes expressed in the tissue as background. Enrichments for genes with conserved sex bias and calculated TWAS Z-score in the same tissue are also provided.

<Excel file >

Table S7.

Sex bias estimates in the cattle pituitary gland, from Seo et al, (2016).

<attached .txt file >

Gene	Species with height/body size association	Conserved sex-biased expression	Cross-tissue TWAS Z-score
LCORL	Humans, cattle, dogs	Female, pituitary gland	-28.7
PLAG1	Humans, cattle	Female, colon	-1.06
CCND2	Humans, cattle	Male, heart	4.43
TTNI21	Humans, cattle		
HMGA2	Humans, cattle, dogs		
TCP11	Humans, cattle		
IGF1	Humans, cattle, dogs		
IGF1R	Humans, dogs		
IGF2BP2	Humans, dogs		
GHR	Humans, dogs		
PLEKHA1	Humans, cattle		
STC2	Humans, cattle, dogs		
INSR	Humans, cattle		
GNA12	Humans, cattle	Female, skin	-120
FBN1	Humans, cattle		
ADAMTS17	Humans, cattle		
DIS3L2	Humans, cattle		
DNMT3A	Humans, cattle		
NOV	Humans, cattle		
FGFR2	Humans, cattle		
FNDC3B	Humans, cattle		
LCOR	Humans, cattle		
LIN28B	Humans, cattle		
PAPPA2	Humans, cattle		
IGF2BP3	Humans, cattle		
SYN3	Humans, cattle		

Table S8: Individual loci with genome-wide significant associations with height in multiple species. Conserved sex bias in expression in specific tissues, as well as cross-tissue TWAS Z-scores calculated as described, are also provided. References for height associations in each species: humans (*57*); cattle (*59*); dogs (*58*).

Table S9.

Information on motifs for sex-biased transcription factors correlated with gains or losses of sex bias.

<Excel file >

References and Notes

1. J. C. K. Wells, Sexual dimorphism of body composition. *Best Pract. Res. Clin. Endocrinol. Metab.* **21**, 415–430 (2007). doi:10.1016/j.beem.2007.04.007 Medline

2. H. J. Green, I. G. Fraser, D. A. Ranney, Male and female differences in enzyme activities of energy metabolism in vastus lateralis muscle. *J. Neurol. Sci.* **65**, 323–331 (1984). doi:10.1016/0022-510X(84)90095-9 Medline

3. A. N. V. Ruigrok, G. Salimi-Khorshidi, M.-C. Lai, S. Baron-Cohen, M. V. Lombardo, R. J. Tait, J. Suckling, A meta-analysis of sex differences in human brain structure. *Neurosci. Biobehav. Rev.* **39**, 34–50 (2014). doi:10.1016/j.neubiorev.2013.12.004 Medline

4. S. L. Klein, K. L. Flanagan, Sex differences in immune responses. *Nat. Rev. Immunol.* **16**, 626–638 (2016). doi:10.1038/nri.2016.90 Medline

5. C. S. Hayward, W. V. Kalnins, R. P. Kelly, Gender-related differences in left ventricular chamber function. *Cardiovasc. Res.* **49**, 340–350 (2001). doi:10.1016/S0008-6363(00)00280-7 Medline

6. S. T. Ngo, F. J. Steyn, P. A. McCombe, Gender differences in autoimmune disease. *Front. Neuroendocrinol.* **35**, 347–369 (2014). doi:10.1016/j.yfrne.2014.04.004 Medline

7. V. Regitz-Zagrosek, S. Oertelt-Prigione, E. Prescott, F. Franconi, E. Gerdts, A. Foryst-Ludwig, A. H. Maas, A. Kautzky-Willer, D. Knappe-Wegner, U. Kintscher, K. H. Ladwig, K. Schenck-Gustafsson, V. Stangl; EUGenMed Cardiovascular Clinical Study Group, Gender in cardiovascular diseases: Impact on clinical manifestations, management, and outcomes. *Eur. Heart J.* **37**, 24–34 (2016). doi:10.1093/eurheartj/ehv598 Medline

8. D. M. Werling, D. H. Geschwind, Sex differences in autism spectrum disorders. *Curr. Opin. Neurol.* **26**, 146–153 (2013). doi:10.1097/WCO.0b013e32835ee548 Medline

9. H. Olson, G. Betton, D. Robinson, K. Thomas, A. Monro, G. Kolaja, P. Lilly, J. Sanders, G. Sipes, W. Bracken, M. Dorato, K. Van Deun, P. Smith, B. Berger, A. Heller, Concordance of the toxicity of pharmaceuticals in humans and in animals. *Regul. Toxicol. Pharmacol.* **32**, 56–67 (2000). doi:10.1006/rtph.2000.1399 Medline

10. P. Lindenfors, J. L. Gittleman, K. Jones, in *Evolutionary Studies of Sexual Size Dimorphism* (Oxford Univ. Press, 2007), pp. 16–26.

11. R. A. Gorski, J. H. Gordon, J. E. Shryne, A. M. Southam, Evidence for a morphological sex difference within the medial preoptic area of the rat brain. *Brain Res.* **148**, 333–346 (1978). doi:10.1016/0006-8993(78)90723-0 Medline

12. R. S. Scotland, M. J. Stables, S. Madalli, P. Watson, D. W. Gilroy, Sex differences in resident immune cell phenotype underlie more efficient acute inflammatory responses in female mice. *Blood* **118**, 5918–5927 (2011). doi:10.1182/blood-2011-03-340281 Medline

13. K. M. Shioura, D. L. Geenen, P. H. Goldspink, Sex-related changes in cardiac function following myocardial infarction in mice. *Am. J. Physiol. Regul. Integr. Comp. Physiol.* **295**, R528–R534 (2008). doi:10.1152/ajpregu.90342.2008 Medline

14. H. Skaletsky, T. Kuroda-Kawaguchi, P. J. Minx, H. S. Cordum, L. Hillier, L. G. Brown, S. Repping, T. Pyntikova, J. Ali, T. Bieri, A. Chinwalla, A. Delehaunty, K. Delehaunty, H. Du, G. Fewell, L. Fulton, R. Fulton, T. Graves, S.-F. Hou, P. Latrielle, S. Leonard, E. Mardis, R. Maupin, J. McPherson, T. Miner, W. Nash, C. Nguyen, P. Ozersky, K. Pepin, S. Rock, T. Rohlfing, K. Scott, B. Schultz, C. Strong, A. Tin-Wollam, S.-P. Yang, R. H. Waterston, R. K. Wilson, S. Rozen, D. C. Page, The male-specific region of the human Y chromosome is a mosaic of discrete sequence classes. *Nature* **423**, 825–837 (2003). doi:10.1038/nature01722 Medline

15. D. W. Bellott, J. F. Hughes, H. Skaletsky, L. G. Brown, T. Pyntikova, T.-J. Cho, N. Koutseva, S. Zaghlul, T. Graves, S. Rock, C. Kremitzki, R. S. Fulton, S. Dugan, Y. Ding, D. Morton, Z. Khan, L. Lewis, C. Buhay, Q. Wang, J. Watt, M. Holder, S. Lee, L. Nazareth, J. Alföldi, S. Rozen, D. M. Muzny, W. C. Warren, R. A. Gibbs, R. K. Wilson, D. C. Page, Mammalian Y chromosomes retain widely expressed dosage-sensitive regulators. *Nature* **508**, 494–499 (2014). doi:10.1038/nature13206 Medline

16. T. Tukiainen, A.-C. Villani, A. Yen, M. A. Rivas, J. L. Marshall, R. Satija, M. Aguirre, L. Gauthier, M. Fleharty, A. Kirby, B. B. Cummings, S. E. Castel, K. J. Karczewski, F. Aguet, A. Byrnes, T. Lappalainen, A. Regev, K. G. Ardlie, N. Hacohen, D. G. MacArthur; GTEx Consortium; Laboratory, Data Analysis &Coordinating Center (LDACC)—Analysis Working Group; Statistical Methods groups—Analysis Working Group; Enhancing GTEx (eGTEx) groups; NIH Common Fund; NIH/NCI; NIH/NHGRI; NIH/NIMH; NIH/NIDA; Biospecimen Collection Source Site—NDRI; Biospecimen Collection Source Site—RPCI; Biospecimen Core Resource—VARI; Brain Bank Repository—University of Miami Brain Endowment Bank; Leidos Biomedical—Project Management; ELSI Study; Genome Browser Data Integration &Visualization—EBI; Genome Browser Data Integration &Visualization—UCSC Genomics Institute, University of California Santa Cruz, Landscape of X chromosome inactivation across human tissues. *Nature* **550**, 244–248 (2017). doi:10.1038/nature24265 Medline

17. M. Melé, P. G. Ferreira, F. Reverter, D. S. DeLuca, J. Monlong, M. Sammeth, T. R. Young, J. M. Goldmann, D. D. Pervouchine, T. J. Sullivan, R. Johnson, A. V. Segrè, S. Djebali, A. Niarchou, F. A. Wright, T. Lappalainen, M. Calvo, G. Getz, E. T. Dermitzakis, K. G. Ardlie, R. Guigó, The human transcriptome across tissues and individuals. *Science* **348**, 660–665 (2015). doi:10.1126/science.aaa0355 Medline

18. M. Gershoni, S. Pietrokovski, The landscape of sex-differential transcriptome and its consequent selection in human adults. *BMC Biol.* **15**, 7 (2017). doi:10.1186/s12915-017-0352-z Medline

19. X. Yang, E. E. Schadt, S. Wang, H. Wang, A. P. Arnold, L. Ingram-Drake, T. A. Drake, A. J. Lusis, Tissue-specific expression and regulation of sexually dimorphic genes in mice. *Genome Res.* **16**, 995–1004 (2006). doi:10.1101/gr.5217506 Medline

20. J. M. Ranz, C. I. Castillo-Davis, C. D. Meiklejohn, D. L. Hartl, Sex-dependent gene expression and evolution of the *Drosophila* transcriptome. *Science* **300**, 1742–1745 (2003). doi:10.1126/science.1085881 Medline

21. Y. Zhang, D. Sturgill, M. Parisi, S. Kumar, B. Oliver, Constraint and turnover in sex-biased gene expression in the genus *Drosophila*. *Nature* **450**, 233–237 (2007). doi:10.1038/nature06323 Medline

22. S. Grath, J. Parsch, Rate of amino acid substitution is influenced by the degree and conservation of male-biased transcription over 50 myr of *Drosophila* evolution. *Genome Biol. Evol.* **4**, 346–359 (2012). doi:10.1093/gbe/evs012 Medline

23. R. Assis, Q. Zhou, D. Bachtrog, Sex-biased transcriptome evolution in *Drosophila*. *Genome Biol. Evol.* **4**, 1189–1200 (2012). doi:10.1093/gbe/evs093 Medline

24. J. C. Perry, P. W. Harrison, J. E. Mank, The ontogeny and evolution of sex-biased gene expression in *Drosophila melanogaster*. *Mol. Biol. Evol.* **31**, 1206–1219 (2014). doi:10.1093/molbev/msu072 Medline

25. B. Reinius, P. Saetre, J. A. Leonard, R. Blekhman, R. Merino-Martinez, Y. Gilad, E. Jazin, An evolutionarily conserved sexual signature in the primate brain. *PLOS Genet.* **4**, e1000100 (2008). doi:10.1371/journal.pgen.1000100 Medline

26. R. Blekhman, J. C. Marioni, P. Zumbo, M. Stephens, Y. Gilad, Sex-specific and lineage-specific alternative splicing in primates. *Genome Res.* **20**, 180–189 (2010). doi:10.1101/gr.099226.109 Medline

27. Y. Liang, L. C. Tsoi, X. Xing, M. A. Beamer, W. R. Swindell, M. K. Sarkar, C. C. Berthier, P. E. Stuart, P. W. Harms, R. P. Nair, J. T. Elder, J. J. Voorhees, J. M. Kahlenberg, J. E. Gudjonsson, A gene network regulated by the transcription factor VGLL3 as a promoter of sex-biased autoimmune diseases. *Nat. Immunol.* **18**, 152–160 (2017). doi:10.1038/ni.3643 Medline

28. A. E. Russi, M. E. Ebel, Y. Yang, M. A. Brown, Male-specific IL-33 expression regulates sex-dimorphic EAE susceptibility. *Proc. Natl. Acad. Sci. U.S.A.* **115**, E1520–E1529 (2018). doi:10.1073/pnas.1710401115 Medline

29. M. Souyris, C. Cenac, P. Azar, D. Daviaud, A. Canivet, S. Grunenwald, C. Pienkowski, J. Chaumeil, J. E. Mejía, J.-C. Guéry, *TLR7* escapes X chromosome inactivation in immune cells. *Sci. Immunol.* **3**, eaap8855 (2018). doi:10.1126/sciimmunol.aap8855 Medline

30. E. A. Boyle, Y. I. Li, J. K. Pritchard, An expanded view of complex traits: From polygenic to omnigenic. *Cell* **169**, 1177–1186 (2017). doi:10.1016/j.cell.2017.05.038 Medline

31. T. M. Williams, J. E. Selegue, T. Werner, N. Gompel, A. Kopp, S. B. Carroll, The regulation and evolution of a genetic switch controlling sexually dimorphic traits in *Drosophila*. *Cell* **134**, 610–623 (2008). doi:10.1016/j.cell.2008.06.052 Medline

32. C. M. Disteche, Dosage compensation of the sex chromosomes. *Annu. Rev. Genet.* **46**, 537–560 (2012). doi:10.1146/annurev-genet-110711-155454 Medline

33. C. M. Disteche, Dosage compensation of the sex chromosomes and autosomes. *Semin. Cell Dev. Biol.* **56**, 9–18 (2016). doi:10.1016/j.semcdb.2016.04.013 Medline

34. Materials and methods are available as supplementary materials.

35. GTEx Consortium, Genetic effects on gene expression across human tissues. *Nature* **550**, 204–213 (2017). doi:10.1038/nature24277 Medline

36. A. M. Newman, C. L. Liu, M. R. Green, A. J. Gentles, W. Feng, Y. Xu, C. D. Hoang, M. Diehn, A. A. Alizadeh, Robust enumeration of cell subsets from tissue expression profiles. *Nat. Methods* **12**, 453–457 (2015). doi:10.1038/nmeth.3337 Medline

37. J. Merkin, C. Russell, P. Chen, C. B. Burge, Evolutionary dynamics of gene and isoform regulation in mammalian tissues. *Science* **338**, 1593–1599 (2012). doi:10.1126/science.1228186 Medline

38. D. Brawand, M. Soumillon, A. Necsulea, P. Julien, G. Csárdi, P. Harrigan, M. Weier, A. Liechti, A. Aximu-Petri, M. Kircher, F. W. Albert, U. Zeller, P. Khaitovich, F. Grützner, S. Bergmann, R. Nielsen, S. Pääbo, H. Kaessmann, The evolution of gene expression levels in mammalian organs. *Nature* **478**, 343–348 (2011). doi:10.1038/nature10532 Medline

39. D. M. Werling, N. N. Parikshak, D. H. Geschwind, Gene expression in human brain implicates sexually dimorphic pathways in autism spectrum disorders. *Nat. Commun.* **7**, 10717 (2016). doi:10.1038/ncomms10717 Medline

40. M. E. Lindholm, M. Huss, B. W. Solnestam, S. Kjellqvist, J. Lundeberg, C. J. Sundberg, The human skeletal muscle transcriptome: Sex differences, alternative splicing, and tissue homogeneity assessed with RNA sequencing. *FASEB J.* **28**, 4571–4581 (2014). doi:10.1096/fj.14-255000 Medline

41. M. S. Newman, T. Nguyen, M. J. Watson, R. W. Hull, H.-G. Yu, Transcriptome profiling reveals novel BMI- and sex-specific gene expression signatures for human cardiac hypertrophy. *Physiol. Genomics* **49**, 355–367 (2017). doi:10.1152/physiolgenomics.00122.2016 Medline

42. N. Viguerie, E. Montastier, J.-J. Maoret, B. Roussel, M. Combes, C. Valle, N. Villa-Vialaneix, J. S. Iacovoni, J. A. Martinez, C. Holst, A. Astrup, H. Vidal, K. Clément, J. Hager, W. H. M. Saris, D. Langin, Determinants of human adipose tissue gene expression: Impact of diet, sex, metabolic status, and cis genetic regulation. *PLOS Genet.* **8**, e1002959 (2012). doi:10.1371/journal.pgen.1002959 Medline

43. R. Marin, D. Cortez, F. Lamanna, M. M. Pradeepa, E. Leushkin, P. Julien, A. Liechti, J. Halbert, T. Brüning, K. Mössinger, T. Trefzer, C. Conrad, H. N. Kerver, J. Wade, P. Tschopp, H. Kaessmann, Convergent origination of a *Drosophila*-like dosage compensation mechanism in a reptile lineage. *Genome Res.* **27**, 1974–1987 (2017). doi:10.1101/gr.223727.117 Medline

44. B. Li, T. Qing, J. Zhu, Z. Wen, Y. Yu, R. Fukumura, Y. Zheng, Y. Gondo, L. Shi, A comprehensive mouse transcriptomic BodyMap across 17 tissues by RNA-seq. *Sci. Rep.* **7**, 4200 (2017). doi:10.1038/s41598-017-04520-z Medline

45. M. D. Franco, F. Colombo, A. Galvan, L. D. Cecco, E. Spada, S. Milani, O. M. Ibanez, T. A. Dragani, Transcriptome of normal lung distinguishes mouse lines with different susceptibility to inflammation and to lung tumorigenesis. *Cancer Lett.* **294**, 187–194 (2010). doi:10.1016/j.canlet.2010.01.038 Medline

46. S. M. Urbut, G. Wang, P. Carbonetto, M. Stephens, Flexible statistical methods for estimating and testing effects in genomic studies with multiple conditions. *Nat. Genet.* **51**, 187–195 (2019). doi:10.1038/s41588-018-0268-8 Medline

47. J. Chen, R. Swofford, J. Johnson, B. B. Cummings, N. Rogel, K. Lindblad-Toh, W. Haerty, F. D. Palma, A. Regev, A quantitative framework for characterizing the evolutionary history of mammalian gene expression. *Genome Res.* **29**, 53–63 (2019). doi:10.1101/gr.237636.118 Medline

48. L. Yengo, J. Sidorenko, K. E. Kemper, Z. Zheng, A. R. Wood, M. N. Weedon, T. M. Frayling, J. Hirschhorn, J. Yang, P. M. Visscher; GIANT Consortium, Meta-analysis of genome-wide association studies for height and body mass index in ~700000 individuals of European ancestry. *Hum. Mol. Genet.* **27**, 3641–3649 (2018). doi:10.1093/hmg/ddy271 Medline

49. T. Tukiainen, M. Pirinen, A.-P. Sarin, C. Ladenvall, J. Kettunen, T. Lehtimäki, M.-L. Lokki, M. Perola, J. Sinisalo, E. Vlachopoulou, J. G. Eriksson, L. Groop, A. Jula, M.-R. Järvelin, O. T. Raitakari, V. Salomaa, S. Ripatti, Chromosome X-wide association study identifies Loci for fasting insulin and height and evidence for incomplete dosage compensation. *PLOS Genet.* **10**, e1004127 (2014). doi:10.1371/journal.pgen.1004127 Medline

50. J. Sidorenko, I. Kassam, K. Kemper, J. Zeng, L. Lloyd-Jones, G. W. Montgomery, G. Gibson, A. Metspalu, T. Esko, J. Yang, A. F. McRae, P. M. Visscher, The effect of X-linked dosage compensation on complex trait variation. bioRxiv 433870 [Preprint]. 3 October 2018. https://doi.org/10.1101/433870.

51. K. Rawlik, O. Canela-Xandri, A. Tenesa, Evidence for sex-specific genetic architectures across a spectrum of human complex traits. *Genome Biol.* **17**, 166 (2016). doi:10.1186/s13059-016-1025-x Medline

52. G. Stulp, L. Barrett, Evolutionary perspectives on human height variation. *Biol. Rev. Camb. Philos. Soc.* **91**, 206–234 (2016). doi:10.1111/brv.12165 Medline

53. J. S. Sanjak, J. Sidorenko, M. R. Robinson, K. R. Thornton, P. M. Visscher, Evidence of directional and stabilizing selection in contemporary humans. *Proc. Natl. Acad. Sci. U.S.A.* **115**, 151–156 (2018). doi:10.1073/pnas.1707227114 Medline

54. A. Gusev, A. Ko, H. Shi, G. Bhatia, W. Chung, B. W. J. H. Penninx, R. Jansen, E. J. C. de Geus, D. I. Boomsma, F. A. Wright, P. F. Sullivan, E. Nikkola, M. Alvarez, M. Civelek, A. J. Lusis, T. Lehtimäki, E. Raitoharju, M. Kähönen, I. Seppälä, O. T. Raitakari, J. Kuusisto, M. Laakso, A. L. Price, P. Pajukanta, B. Pasaniuc, Integrative approaches for large-scale transcriptome-wide association studies. *Nat. Genet.* **48**, 245–252 (2016). doi:10.1038/ng.3506 Medline

55. J. MacArthur, E. Bowler, M. Cerezo, L. Gil, P. Hall, E. Hastings, H. Junkins, A. McMahon, A. Milano, J. Morales, Z. M. Pendlington, D. Welter, T. Burdett, L. Hindorff, P. Flicek, F. Cunningham, H. Parkinson, The new NHGRI-EBI Catalog of published genome-wide association studies (GWAS Catalog). *Nucleic Acids Res.* **45** (D1), D896–D901 (2017). doi:10.1093/nar/gkw1133 Medline

56. P. R. Loh, G. Kichaev, S. Gazal, A. P. Schoech, A. L. Price, Mixed-model association for biobank-scale datasets. *Nat. Genet.* **50**, 906–908 (2018). doi:10.1038/s41588-018-0144-6 Medline

57. A. R. Wood, T. Esko, J. Yang, S. Vedantam, T. H. Pers, S. Gustafsson, A. Y. Chu, K. Estrada, J. Luan, Z. Kutalik, N. Amin, M. L. Buchkovich, D. C. Croteau-Chonka, F. R.

Day, Y. Duan, T. Fall, R. Fehrmann, T. Ferreira, A. U. Jackson, J. Karjalainen, K. S. Lo, A. E. Locke, R. Mägi, E. Mihailov, E. Porcu, J. C. Randall, A. Scherag, A. A. E. Vinkhuyzen, H.-J. Westra, T. W. Winkler, T. Workalemahu, J. H. Zhao, D. Absher, E. Albrecht, D. Anderson, J. Baron, M. Beekman, A. Demirkan, G. B. Ehret, B. Feenstra, M. F. Feitosa, K. Fischer, R. M. Fraser, A. Goel, J. Gong, A. E. Justice, S. Kanoni, M. E. Kleber, K. Kristiansson, U. Lim, V. Lotay, J. C. Lui, M. Mangino, I. Mateo Leach, C. Medina-Gomez, M. A. Nalls, D. R. Nyholt, C. D. Palmer, D. Pasko, S. Pechlivanis, I. Prokopenko, J. S. Ried, S. Ripke, D. Shungin, A. Stancáková, R. J. Strawbridge, Y. J. Sung, T. Tanaka, A. Teumer, S. Trompet, S. W. van der Laan, J. van Setten, J. V. Van Vliet-Ostaptchouk, Z. Wang, L. Yengo, W. Zhang, U. Afzal, J. Arnlöv, G. M. Arscott, S. Bandinelli, A. Barrett, C. Bellis, A. J. Bennett, C. Berne, M. Blüher, J. L. Bolton, Y. Böttcher, H. A. Boyd, M. Bruinenberg, B. M. Buckley, S. Buyske, I. H. Caspersen, P. S. Chines, R. Clarke, S. Claudi-Boehm, M. Cooper, E. W. Daw, P. A. De Jong, J. Deelen, G. Delgado, J. C. Denny, R. Dhonukshe-Rutten, M. Dimitriou, A. S. F. Doney, M. Dörr, N. Eklund, E. Eury, L. Folkersen, M. E. Garcia, F. Geller, V. Giedraitis, A. S. Go, H. Grallert, T. B. Grammer, J. Gräßler, H. Grönberg, L. C. P. G. M. de Groot, C. J. Groves, J. Haessler, P. Hall, T. Haller, G. Hallmans, A. Hannemann, C. A. Hartman, M. Hassinen, C. Hayward, N. L. Heard-Costa, Q. Helmer, G. Hemani, A. K. Henders, H. L. Hillege, M. A. Hlatky, W. Hoffmann, P. Hoffmann, O. Holmen, J. J. Houwing-Duistermaat, T. Illig, A. Isaacs, A. L. James, J. Jeff, B. Johansen, Å. Johansson, J. Jolley, T. Juliusdottir, J. Junttila, A. N. Kho, L. Kinnunen, N. Klopp, T. Kocher, W. Kratzer, P. Lichtner, L. Lind, J. Lindström, S. Lobbens, M. Lorentzon, Y. Lu, V. Lyssenko, P. K. E. Magnusson, A. Mahajan, M. Maillard, W. L. McArdle, C. A. McKenzie, S. McLachlan, P. J. McLaren, C. Menni, S. Merger, L. Milani, A. Moayyeri, K. L. Monda, M. A. Morken, G. Müller, M. Müller-Nurasyid, A. W. Musk, N. Narisu, M. Nauck, I. M. Nolte, M. M. Nöthen, L. Oozageer, S. Pilz, N. W. Rayner, F. Renstrom, N. R. Robertson, L. M. Rose, R. Roussel, S. Sanna, H. Scharnagl, S. Scholtens, F. R. Schumacher, H. Schunkert, R. A. Scott, J. Sehmi, T. Seufferlein, J. Shi, K. Silventoinen, J. H. Smit, A. V. Smith, J. Smolonska, A. V. Stanton, K. Stirrups, D. J. Stott, H. M. Stringham, J. Sundström, M. A. Swertz, A.-C. Syvänen, B. O. Tayo, G. Thorleifsson, J. P. Tyrer, S. van Dijk, N. M. van Schoor, N. van der Velde, D. van Heemst, F. V. A. van Oort, S. H. Vermeulen, N. Verweij, J. M. Vonk, L. L. Waite, M. Waldenberger, R. Wennauer, L. R. Wilkens, C. Willenborg, T. Wilsgaard, M. K. Wojczynski, A. Wong, A. F. Wright, Q. Zhang, D. Arveiler, S. J. L. Bakker, J. Beilby, R. N. Bergman, S. Bergmann, R. Biffar, J. Blangero, D. I. Boomsma, S. R. Bornstein, P. Bovet, P. Brambilla, M. J. Brown, H. Campbell, M. J. Caulfield, A. Chakravarti, R. Collins, F. S. Collins, D. C. Crawford, L. A. Cupples, J. Danesh, U. de Faire, H. M. den Ruijter, R. Erbel, J. Erdmann, J. G. Eriksson, M. Farrall, E. Ferrannini, J. Ferrières, I. Ford, N. G. Forouhi, T. Forrester, R. T. Gansevoort, P. V. Gejman, C. Gieger, A. Golay, O. Gottesman, V. Gudnason, U. Gyllensten, D. W. Haas, A. S. Hall, T. B. Harris, A. T. Hattersley, A. C. Heath, C. Hengstenberg, A. A. Hicks, L. A. Hindorff, A. D. Hingorani, A. Hofman, G. K. Hovingh, S. E. Humphries, S. C. Hunt, E. Hypponen, K. B. Jacobs, M.-R. Jarvelin, P. Jousilahti, A. M. Jula, J. Kaprio, J. J. P. Kastelein, M. Kayser, F. Kee, S. M. Keinanen-Kiukaanniemi, L. A. Kiemeney, J. S. Kooner, C. Kooperberg, S. Koskinen, P. Kovacs, A. T. Kraja, M. Kumari, J. Kuusisto, T. A. Lakka, C. Langenberg, L. Le Marchand, T. Lehtimäki, S. Lupoli, P. A. F. Madden, S. Männistö, P. Manunta, A. Marette, T. C. Matise, B. McKnight, T. Meitinger, F. L. Moll,

G. W. Montgomery, A. D. Morris, A. P. Morris, J. C. Murray, M. Nelis, C. Ohlsson, A. J. Oldehinkel, K. K. Ong, W. H. Ouwehand, G. Pasterkamp, A. Peters, P. P. Pramstaller, J. F. Price, L. Qi, O. T. Raitakari, T. Rankinen, D. C. Rao, T. K. Rice, M. Ritchie, I. Rudan, V. Salomaa, N. J. Samani, J. Saramies, M. A. Sarzynski, P. E. H. Schwarz, S. Sebert, P. Sever, A. R. Shuldiner, J. Sinisalo, V. Steinthorsdottir, R. P. Stolk, J.-C. Tardif, A. Tönjes, A. Tremblay, E. Tremoli, J. Virtamo, M.-C. Vohl, P. Amouyel, F. W. Asselbergs, T. L. Assimes, M. Bochud, B. O. Boehm, E. Boerwinkle, E. P. Bottinger, C. Bouchard, S. Cauchi, J. C. Chambers, S. J. Chanock, R. S. Cooper, P. I. W. de Bakker, G. Dedoussis, L. Ferrucci, P. W. Franks, P. Froguel, L. C. Groop, C. A. Haiman, A. Hamsten, M. G. Hayes, J. Hui, D. J. Hunter, K. Hveem, J. W. Jukema, R. C. Kaplan, M. Kivimaki, D. Kuh, M. Laakso, Y. Liu, N. G. Martin, W. März, M. Melbye, S. Moebus, P. B. Munroe, I. Njølstad, B. A. Oostra, C. N. A. Palmer, N. L. Pedersen, M. Perola, L. Pérusse, U. Peters, J. E. Powell, C. Power, T. Quertermous, R. Rauramaa, E. Reinmaa, P. M. Ridker, F. Rivadeneira, J. I. Rotter, T. E. Saaristo, D. Saleheen, D. Schlessinger, P. E. Slagboom, H. Snieder, T. D. Spector, K. Strauch, M. Stumvoll, J. Tuomilehto, M. Uusitupa, P. van der Harst, H. Völzke, M. Walker, N. J. Wareham, H. Watkins, H.-E. Wichmann, J. F. Wilson, P. Zanen, P. Deloukas, I. M. Heid, C. M. Lindgren, K. L. Mohlke, E. K. Speliotes, U. Thorsteinsdottir, I. Barroso, C. S. Fox, K. E. North, D. P. Strachan, J. S. Beckmann, S. I. Berndt, M. Boehnke, I. B. Borecki, M. I. McCarthy, A. Metspalu, K. Stefansson, A. G. Uitterlinden, C. M. van Duijn, L. Franke, C. J. Willer, A. L. Price, G. Lettre, R. J. F. Loos, M. N. Weedon, E. Ingelsson, J. R. O'Connell, G. R. Abecasis, D. I. Chasman, M. E. Goddard, P. M. Visscher, J. N. Hirschhorn, T. M. Frayling; Electronic Medical Records and Genomics (eMEMERGEGE) Consortium; MIGen Consortium; PAGEGE Consortium; LifeLines Cohort Study, Defining the role of common variation in the genomic and biological architecture of adult human height. *Nat. Genet.* **46**, 1173–1186 (2014). doi:10.1038/ng.3097 Medline

58. J. J. Hayward, M. G. Castelhano, K. C. Oliveira, E. Corey, C. Balkman, T. L. Baxter, M. L. Casal, S. A. Center, M. Fang, S. J. Garrison, S. E. Kalla, P. Korniliev, M. I. Kotlikoff, N. S. Moise, L. M. Shannon, K. W. Simpson, N. B. Sutter, R. J. Todhunter, A. R. Boyko, Complex disease and phenotype mapping in the domestic dog. *Nat. Commun.* **7**, 10460 (2016). doi:10.1038/ncomms10460 Medline

59. A. C. Bouwman, H. D. Daetwyler, A. J. Chamberlain, C. H. Ponce, M. Sargolzaei, F. S. Schenkel, G. Sahana, A. Govignon-Gion, S. Boitard, M. Dolezal, H. Pausch, R. F. Brøndum, P. J. Bowman, B. Thomsen, B. Guldbrandtsen, M. S. Lund, B. Servin, D. J. Garrick, J. Reecy, J. Vilkki, A. Bagnato, M. Wang, J. L. Hoff, R. D. Schnabel, J. F. Taylor, A. A. E. Vinkhuyzen, F. Panitz, C. Bendixen, L.-E. Holm, B. Gredler, C. Hozé, M. Boussaha, M.-P. Sanchez, D. Rocha, A. Capitan, T. Tribout, A. Barbat, P. Croiseau, C. Drögemüller, V. Jagannathan, C. Vander Jagt, J. J. Crowley, A. Bieber, D. C. Purfield, D. P. Berry, R. Emmerling, K.-U. Götz, M. Frischknecht, I. Russ, J. Sölkner, C. P. Van Tassell, R. Fries, P. Stothard, R. F. Veerkamp, D. Boichard, M. E. Goddard, B. J. Hayes, Meta-analysis of genome-wide association studies for cattle stature identifies common genes that regulate body size in mammals. *Nat. Genet.* **50**, 362–367 (2018). doi:10.1038/s41588-018-0056-5 Medline

60. H. Signer-Hasler, C. Flury, B. Haase, D. Burger, H. Simianer, T. Leeb, S. Rieder, A genome-wide association study reveals loci influencing height and other conformation traits in horses. *PLOS ONE* **7**, e37282 (2012). doi:10.1371/journal.pone.0037282 Medline

61. M. Seo, K. Caetano-Anolles, S. Rodriguez-Zas, S. Ka, J. Y. Jeong, S. Park, M. J. Kim, W.-G. Nho, S. Cho, H. Kim, H.-J. Lee, Comprehensive identification of sexually dimorphic genes in diverse cattle tissues using RNA-seq. *BMC Genomics* **17**, 81 (2016). doi:10.1186/s12864-016-2400-4 Medline

62. J. Metzger, R. Schrimpf, U. Philipp, O. Distl, Expression levels of LCORL are associated with body size in horses. *PLOS ONE* **8**, e56497 (2013). doi:10.1371/journal.pone.0056497 Medline

63. N. Stroth, Y. Holighaus, D. Ait-Ali, L. E. Eiden, PACAP: A master regulator of neuroendocrine stress circuits and the cellular stress response. *Ann. N. Y. Acad. Sci.* **1220**, 49–59 (2011). doi:10.1111/j.1749-6632.2011.05904.x Medline

64. T. Kanzleiter, M. Rath, D. Penkov, D. Puchkov, N. Schulz, F. Blasi, A. Schürmann, Pknox1/Prep1 regulates mitochondrial oxidative phosphorylation components in skeletal muscle. *Mol. Cell. Biol.* **34**, 290–298 (2014). doi:10.1128/MCB.01232-13 Medline

65. K. S. Small, M. Todorčević, M. Civelek, J. S. El-Sayed Moustafa, X. Wang, M. M. Simon, J. Fernandez-Tajes, A. Mahajan, M. Horikoshi, A. Hugill, C. A. Glastonbury, L. Quaye, M. J. Neville, S. Sethi, M. Yon, C. Pan, N. Che, A. Viñuela, P.-C. Tsai, A. Nag, A. Buil, G. Thorleifsson, A. Raghavan, Q. Ding, A. P. Morris, J. T. Bell, U. Thorsteinsdottir, K. Stefansson, M. Laakso, I. Dahlman, P. Arner, A. L. Gloyn, K. Musunuru, A. J. Lusis, R. D. Cox, F. Karpe, M. I. McCarthy, Regulatory variants at KLF14 influence type 2 diabetes risk via a female-specific effect on adipocyte size and body composition. *Nat. Genet.* **50**, 572–580 (2018). doi:10.1038/s41588-018-0088-x Medline

66. J. Yang, B. Benyamin, B. P. McEvoy, S. Gordon, A. K. Henders, D. R. Nyholt, P. A. Madden, A. C. Heath, N. G. Martin, G. W. Montgomery, M. E. Goddard, P. M. Visscher, Common SNPs explain a large proportion of the heritability for human height. *Nat. Genet.* **42**, 565–569 (2010). doi:10.1038/ng.608 Medline

67. E. Rao, B. Weiss, M. Fukami, A. Rump, B. Niesler, A. Mertz, K. Muroya, G. Binder, S. Kirsch, M. Winkelmann, G. Nordsiek, U. Heinrich, M. H. Breuning, M. B. Ranke, A. Rosenthal, T. Ogata, G. A. Rappold, Pseudoautosomal deletions encompassing a novel homeobox gene cause growth failure in idiopathic short stature and Turner syndrome. *Nat. Genet.* **16**, 54–63 (1997). doi:10.1038/ng0597-54 Medline

68. T. Ogata, N. Matsuo, Sex chromosome aberrations and stature: Deduction of the principal factors involved in the determination of adult height. *Hum. Genet.* **91**, 551–562 (1993). doi:10.1007/BF00205079 Medline

69. A. K. San Roman, D. C. Page, A strategic research alliance: Turner syndrome and sex differences. *Am. J. Med. Genet. C. Semin. Med. Genet.* **181**, 59–67 (2019). doi:10.1002/ajmg.c.31677 Medline

70. J. Parsch, H. Ellegren, The evolutionary causes and consequences of sex-biased gene expression. *Nat. Rev. Genet.* **14**, 83–87 (2013). doi:10.1038/nrg3376 Medline

71. F. Ruzicka, M. S. Hill, T. M. Pennell, I. Flis, F. C. Ingleby, R. Mott, K. Fowler, E. H. Morrow, M. Reuter, Genome-wide sexually antagonistic variants reveal long-standing constraints on sexual dimorphism in fruit flies. *PLOS Biol.* **17**, e3000244 (2019). doi:10.1371/journal.pbio.3000244 Medline

72. J. C. Randall, T. W. Winkler, Z. Kutalik, S. I. Berndt, A. U. Jackson, K. L. Monda, T. O. Kilpeläinen, T. Esko, R. Mägi, S. Li, T. Workalemahu, M. F. Feitosa, D. C. Croteau-Chonka, F. R. Day, T. Fall, T. Ferreira, S. Gustafsson, A. E. Locke, I. Mathieson, A. Scherag, S. Vedantam, A. R. Wood, L. Liang, V. Steinthorsdottir, G. Thorleifsson, E. T. Dermitzakis, A. S. Dimas, F. Karpe, J. L. Min, G. Nicholson, D. J. Clegg, T. Person, J. P. Krohn, S. Bauer, C. Buechler, K. Eisinger, A. Bonnefond, P. Froguel, J. J. Hottenga, I. Prokopenko, L. L. Waite, T. B. Harris, A. V. Smith, A. R. Shuldiner, W. L. McArdle, M. J. Caulfield, P. B. Munroe, H. Grönberg, Y. D. Chen, G. Li, J. S. Beckmann, T. Johnson, U. Thorsteinsdottir, M. Teder-Laving, K. T. Khaw, N. J. Wareham, J. H. Zhao, N. Amin, B. A. Oostra, A. T. Kraja, M. A. Province, L. A. Cupples, N. L. Heard-Costa, J. Kaprio, S. Ripatti, I. Surakka, F. S. Collins, J. Saramies, J. Tuomilehto, A. Jula, V. Salomaa, J. Erdmann, C. Hengstenberg, C. Loley, H. Schunkert, C. Lamina, H. E. Wichmann, E. Albrecht, C. Gieger, A. A. Hicks, A. Johansson, P. P. Pramstaller, S. Kathiresan, E. K. Speliotes, B. Penninx, A. L. Hartikainen, M. R. Jarvelin, U. Gyllensten, D. I. Boomsma, H. Campbell, J. F. Wilson, S. J. Chanock, M. Farrall, A. Goel, C. Medina-Gomez, F. Rivadeneira, K. Estrada, A. G. Uitterlinden, A. Hofman, M. C. Zillikens, M. den Heijer, L. A. Kiemeney, A. Maschio, P. Hall, J. Tyrer, A. Teumer, H. Völzke, P. Kovacs, A. Tönjes, M. Mangino, T. D. Spector, C. Hayward, I. Rudan, A. S. Hall, N. J. Samani, A. P. Attwood, J. G. Sambrook, J. Hung, L. J. Palmer, M. L. Lokki, J. Sinisalo, G. Boucher, H. Huikuri, M. Lorentzon, C. Ohlsson, N. Eklund, J. G. Eriksson, C. Barlassina, C. Rivolta, I. M. Nolte, H. Snieder, M. M. Van der Klauw, J. V. Van Vliet-Ostaptchouk, P. V. Gejman, J. Shi, K. B. Jacobs, Z. Wang, S. J. Bakker, I. Mateo Leach, G. Navis, P. van der Harst, N. G. Martin, S. E. Medland, G. W. Montgomery, J. Yang, D. I. Chasman, P. M. Ridker, L. M. Rose, T. Lehtimäki, O. Raitakari, D. Absher, C. Iribarren, H. Basart, K. G. Hovingh, E. Hyppönen, C. Power, D. Anderson, J. P. Beilby, J. Hui, J. Jolley, H. Sager, S. R. Bornstein, P. E. Schwarz, K. Kristiansson, M. Perola, J. Lindström, A. J. Swift, M. Uusitupa, M. Atalay, T. A. Lakka, R. Rauramaa, J. L. Bolton, G. Fowkes, R. M. Fraser, J. F. Price, K. Fischer, K. Krjutå Kov, A. Metspalu, E. Mihailov, C. Langenberg, J. Luan, K. K. Ong, P. S. Chines, S. M. Keinanen-Kiukaanniemi, T. E. Saaristo, S. Edkins, P. W. Franks, G. Hallmans, D. Shungin, A. D. Morris, C. N. Palmer, R. Erbel, S. Moebus, M. M. Nöthen, S. Pechlivanis, K. Hveem, N. Narisu, A. Hamsten, S. E. Humphries, R. J. Strawbridge, E. Tremoli, H. Grallert, B. Thorand, T. Illig, W. Koenig, M. Müller-Nurasyid, A. Peters, B. O. Boehm, M. E. Kleber, W. März, B. R. Winkelmann, J. Kuusisto, M. Laakso, D. Arveiler, G. Cesana, K. Kuulasmaa, J. Virtamo, J. W. Yarnell, D. Kuh, A. Wong, L. Lind, U. de Faire, B. Gigante, P. K. Magnusson, N. L. Pedersen, G. Dedoussis, M. Dimitriou, G. Kolovou, S. Kanoni, K. Stirrups, L. L. Bonnycastle, I. Njølstad, T. Wilsgaard, A. Ganna, E. Rehnberg, A. Hingorani, M. Kivimaki, M. Kumari, T. L. Assimes, I. Barroso, M. Boehnke, I. B. Borecki, P. Deloukas, C. S. Fox, T. Frayling, L. C. Groop, T. Haritunians, D. Hunter, E. Ingelsson, R. Kaplan, K. L. Mohlke, J. R. O'Connell, D. Schlessinger, D. P. Strachan, K. Stefansson, C. M. van Duijn, G. R. Abecasis, M. I. McCarthy, J. N. Hirschhorn, L. Qi, R. J. Loos, C. M. Lindgren, K. E. North, I. M. Heid; DIAGRAM Consortium; MAGIC

Investigators, Sex-stratified genome-wide association studies including 270,000 individuals show sexual dimorphism in genetic loci for anthropometric traits. *PLOS Genet.* **9**, e1003500 (2013). doi:10.1371/journal.pgen.1003500 Medline

73. T. W. Winkler, A. E. Justice, M. Graff, L. Barata, M. F. Feitosa, S. Chu, J. Czajkowski, T. Esko, T. Fall, T. O. Kilpeläinen, Y. Lu, R. Mägi, E. Mihailov, T. H. Pers, S. Rüeger, A. Teumer, G. B. Ehret, T. Ferreira, N. L. Heard-Costa, J. Karjalainen, V. Lagou, A. Mahajan, M. D. Neinast, I. Prokopenko, J. Simino, T. M. Teslovich, R. Jansen, H.-J. Westra, C. C. White, D. Absher, T. S. Ahluwalia, S. Ahmad, E. Albrecht, A. C. Alves, J. L. Bragg-Gresham, A. J. M. de Craen, J. C. Bis, A. Bonnefond, G. Boucher, G. Cadby, Y.-C. Cheng, C. W. K. Chiang, G. Delgado, A. Demirkan, N. Dueker, N. Eklund, G. Eiriksdottir, J. Eriksson, B. Feenstra, K. Fischer, F. Frau, T. E. Galesloot, F. Geller, A. Goel, M. Gorski, T. B. Grammer, S. Gustafsson, S. Haitjema, J.-J. Hottenga, J. E. Huffman, A. U. Jackson, K. B. Jacobs, Å. Johansson, M. Kaakinen, M. E. Kleber, J. Lahti, I. Mateo Leach, B. Lehne, Y. Liu, K. S. Lo, M. Lorentzon, J. Luan, P. A. F. Madden, M. Mangino, B. McKnight, C. Medina-Gomez, K. L. Monda, M. E. Montasser, G. Müller, M. Müller-Nurasyid, I. M. Nolte, K. Panoutsopoulou, L. Pascoe, L. Paternoster, N. W. Rayner, F. Renström, F. Rizzi, L. M. Rose, K. A. Ryan, P. Salo, S. Sanna, H. Scharnagl, J. Shi, A. V. Smith, L. Southam, A. Stančáková, V. Steinthorsdottir, R. J. Strawbridge, Y. J. Sung, I. Tachmazidou, T. Tanaka, G. Thorleifsson, S. Trompet, N. Pervjakova, J. P. Tyrer, L. Vandenput, S. W. van der Laan, N. van der Velde, J. van Setten, J. V. van Vliet-Ostaptchouk, N. Verweij, E. Vlachopoulou, L. L. Waite, S. R. Wang, Z. Wang, S. H. Wild, C. Willenborg, J. F. Wilson, A. Wong, J. Yang, L. Yengo, L. M. Yerges-Armstrong, L. Yu, W. Zhang, J. H. Zhao, E. A. Andersson, S. J. L. Bakker, D. Baldassarre, K. Banasik, M. Barcella, C. Barlassina, C. Bellis, P. Benaglio, J. Blangero, M. Blüher, F. Bonnet, L. L. Bonnycastle, H. A. Boyd, M. Bruinenberg, A. S. Buchman, H. Campbell, Y.-D. I. Chen, P. S. Chines, S. Claudi-Boehm, J. Cole, F. S. Collins, E. J. C. de Geus, L. C. P. G. M. de Groot, M. Dimitriou, J. Duan, S. Enroth, E. Eury, A.-E. Farmaki, N. G. Forouhi, N. Friedrich, P. V. Gejman, B. Gigante, N. Glorioso, A. S. Go, O. Gottesman, J. Gräßler, H. Grallert, N. Grarup, Y.-M. Gu, L. Broer, A. C. Ham, T. Hansen, T. B. Harris, C. A. Hartman, M. Hassinen, N. Hastie, A. T. Hattersley, A. C. Heath, A. K. Henders, D. Hernandez, H. Hillege, O. Holmen, K. G. Hovingh, J. Hui, L. L. Husemoen, N. Hutri-Kähönen, P. G. Hysi, T. Illig, P. L. De Jager, S. Jalilzadeh, T. Jørgensen, J. W. Jukema, M. Juonala, S. Kanoni, M. Karaleftheri, K. T. Khaw, L. Kinnunen, S. J. Kittner, W. Koenig, I. Kolcic, P. Kovacs, N. T. Krarup, W. Kratzer, J. Krüger, D. Kuh, M. Kumari, T. Kyriakou, C. Langenberg, L. Lannfelt, C. Lanzani, V. Lotay, L. J. Launer, K. Leander, J. Lindström, A. Linneberg, Y.-P. Liu, S. Lobbens, R. Luben, V. Lyssenko, S. Männistö, P. K. Magnusson, W. L. McArdle, C. Menni, S. Merger, L. Milani, G. W. Montgomery, A. P. Morris, N. Narisu, M. Nelis, K. K. Ong, A. Palotie, L. Pérusse, I. Pichler, M. G. Pilia, A. Pouta, M. Rheinberger, R. Ribel-Madsen, M. Richards, K. M. Rice, T. K. Rice, C. Rivolta, V. Salomaa, A. R. Sanders, M. A. Sarzynski, S. Scholtens, R. A. Scott, W. R. Scott, S. Sebert, S. Sengupta, B. Sennblad, T. Seufferlein, A. Silveira, P. E. Slagboom, J. H. Smit, T. H. Sparsø, K. Stirrups, R. P. Stolk, H. M. Stringham, M. A. Swertz, A. J. Swift, A.-C. Syvänen, S.-T. Tan, B. Thorand, A. Tönjes, A. Tremblay, E. Tsafantakis, P. J. van der Most, U. Völker, M.-C. Vohl, J. M. Vonk, M. Waldenberger, R. W. Walker, R. Wennauer, E. Widén, G. Willemsen, T. Wilsgaard, A. F. Wright, M. C. Zillikens, S. C. van Dijk, N. M. van

Schoor, F. W. Asselbergs, P. I. W. de Bakker, J. S. Beckmann, J. Beilby, D. A. Bennett, R. N. Bergman, S. Bergmann, C. A. Böger, B. O. Boehm, E. Boerwinkle, D. I. Boomsma, S. R. Bornstein, E. P. Bottinger, C. Bouchard, J. C. Chambers, S. J. Chanock, D. I. Chasman, F. Cucca, D. Cusi, G. Dedoussis, J. Erdmann, J. G. Eriksson, D. A. Evans, U. de Faire, M. Farrall, L. Ferrucci, I. Ford, L. Franke, P. W. Franks, P. Froguel, R. T. Gansevoort, C. Gieger, H. Grönberg, V. Gudnason, U. Gyllensten, P. Hall, A. Hamsten, P. van der Harst, C. Hayward, M. Heliövaara, C. Hengstenberg, A. A. Hicks, A. Hingorani, A. Hofman, F. Hu, H. V. Huikuri, K. Hveem, A. L. James, J. M. Jordan, A. Jula, M. Kähönen, E. Kajantie, S. Kathiresan, L. A. L. M. Kiemeney, M. Kivimaki, P. B. Knekt, H. A. Koistinen, J. S. Kooner, S. Koskinen, J. Kuusisto, W. Maerz, N. G. Martin, M. Laakso, T. A. Lakka, T. Lehtimäki, G. Lettre, D. F. Levinson, L. Lind, M.-L. Lokki, P. Mäntyselkä, M. Melbye, A. Metspalu, B. D. Mitchell, F. L. Moll, J. C. Murray, A. W. Musk, M. S. Nieminen, I. Njølstad, C. Ohlsson, A. J. Oldehinkel, B. A. Oostra, L. J. Palmer, J. S. Pankow, G. Pasterkamp, N. L. Pedersen, O. Pedersen, B. W. Penninx, M. Perola, A. Peters, O. Polašek, P. P. Pramstaller, B. M. Psaty, L. Qi, T. Quertermous, O. T. Raitakari, T. Rankinen, R. Rauramaa, P. M. Ridker, J. D. Rioux, F. Rivadeneira, J. I. Rotter, I. Rudan, H. M. den Ruijter, J. Saltevo, N. Sattar, H. Schunkert, P. E. H. Schwarz, A. R. Shuldiner, J. Sinisalo, H. Snieder, T. I. A. Sørensen, T. D. Spector, J. A. Staessen, B. Stefania, U. Thorsteinsdottir, M. Stumvoll, J.-C. Tardif, E. Tremoli, J. Tuomilehto, A. G. Uitterlinden, M. Uusitupa, A. L. M. Verbeek, S. H. Vermeulen, J. S. Viikari, V. Vitart, H. Völzke, P. Vollenweider, G. Waeber, M. Walker, H. Wallaschofski, N. J. Wareham, H. Watkins, E. Zeggini, A. Chakravarti, D. J. Clegg, L. A. Cupples, P. Gordon-Larsen, C. E. Jaquish, D. C. Rao, G. R. Abecasis, T. L. Assimes, I. Barroso, S. I. Berndt, M. Boehnke, P. Deloukas, C. S. Fox, L. C. Groop, D. J. Hunter, E. Ingelsson, R. C. Kaplan, M. I. McCarthy, K. L. Mohlke, J. R. O'Connell, D. Schlessinger, D. P. Strachan, K. Stefansson, C. M. van Duijn, J. N. Hirschhorn, C. M. Lindgren, I. M. Heid, K. E. North, I. B. Borecki, Z. Kutalik, R. J. F. Loos; CHARGE Consortium; DIAGRAM Consortium; GLGC Consortium; Global-BPGen Consortium; ICBP Consortium; MAGIC Consortium, The influence of age and sex on genetic associations with adult body size and shape: A large-scale genome-wide interaction study. *PLOS Genet.* **11**, e1005378 (2015). doi:10.1371/journal.pgen.1005378 Medline

74. D. Shungin, T. W. Winkler, D. C. Croteau-Chonka, T. Ferreira, A. E. Locke, R. Mägi, R. J. Strawbridge, T. H. Pers, K. Fischer, A. E. Justice, T. Workalemahu, J. M. W. Wu, M. L. Buchkovich, N. L. Heard-Costa, T. S. Roman, A. W. Drong, C. Song, S. Gustafsson, F. R. Day, T. Esko, T. Fall, Z. Kutalik, J. Luan, J. C. Randall, A. Scherag, S. Vedantam, A. R. Wood, J. Chen, R. Fehrmann, J. Karjalainen, B. Kahali, C.-T. Liu, E. M. Schmidt, D. Absher, N. Amin, D. Anderson, M. Beekman, J. L. Bragg-Gresham, S. Buyske, A. Demirkan, G. B. Ehret, M. F. Feitosa, A. Goel, A. U. Jackson, T. Johnson, M. E. Kleber, K. Kristiansson, M. Mangino, I. M. Leach, C. Medina-Gomez, C. D. Palmer, D. Pasko, S. Pechlivanis, M. J. Peters, I. Prokopenko, A. Stančáková, Y. J. Sung, T. Tanaka, A. Teumer, J. V. Van Vliet-Ostaptchouk, L. Yengo, W. Zhang, E. Albrecht, J. Ärnlöv, G. M. Arscott, S. Bandinelli, A. Barrett, C. Bellis, A. J. Bennett, C. Berne, M. Blüher, S. Böhringer, F. Bonnet, Y. Böttcher, M. Bruinenberg, D. B. Carba, I. H. Caspersen, R. Clarke, E. W. Daw, J. Deelen, E. Deelman, G. Delgado, A. S. F. Doney, N. Eklund, M. R. Erdos, K. Estrada, E. Eury, N. Friedrich, M. E. Garcia, V. Giedraitis, B. Gigante, A. S. Go, A. Golay, H. Grallert, T. B. Grammer, J. Gräßler, J. Grewal, C. J. Groves, T. Haller,

G. Hallmans, C. A. Hartman, M. Hassinen, C. Hayward, K. Heikkilä, K.-H. Herzig, Q. Helmer, H. L. Hillege, O. Holmen, S. C. Hunt, A. Isaacs, T. Ittermann, A. L. James, I. Johansson, T. Juliusdottir, I.-P. Kalafati, L. Kinnunen, W. Koenig, I. K. Kooner, W. Kratzer, C. Lamina, K. Leander, N. R. Lee, P. Lichtner, L. Lind, J. Lindström, S. Lobbens, M. Lorentzon, F. Mach, P. K. E. Magnusson, A. Mahajan, W. L. McArdle, C. Menni, S. Merger, E. Mihailov, L. Milani, R. Mills, A. Moayyeri, K. L. Monda, S. P. Mooijaart, T. W. Mühleisen, A. Mulas, G. Müller, M. Müller-Nurasyid, R. Nagaraja, M. A. Nalls, N. Narisu, N. Glorioso, I. M. Nolte, M. Olden, N. W. Rayner, F. Renstrom, J. S. Ried, N. R. Robertson, L. M. Rose, S. Sanna, H. Scharnagl, S. Scholtens, B. Sennblad, T. Seufferlein, C. M. Sitlani, A. V. Smith, K. Stirrups, H. M. Stringham, J. Sundström, M. A. Swertz, A. J. Swift, A.-C. Syvänen, B. O. Tayo, B. Thorand, G. Thorleifsson, A. Tomaschitz, C. Troffa, F. V. A. van Oort, N. Verweij, J. M. Vonk, L. L. Waite, R. Wennauer, T. Wilsgaard, M. K. Wojczynski, A. Wong, Q. Zhang, J. H. Zhao, E. P. Brennan, M. Choi, P. Eriksson, L. Folkersen, A. Franco-Cereceda, A. G. Gharavi, Å. K. Hedman, M.-F. Hivert, J. Huang, S. Kanoni, F. Karpe, S. Keildson, K. Kiryluk, L. Liang, R. P. Lifton, B. Ma, A. J. McKnight, R. McPherson, A. Metspalu, J. L. Min, M. F. Moffatt, G. W. Montgomery, J. M. Murabito, G. Nicholson, D. R. Nyholt, C. Olsson, J. R. B. Perry, E. Reinmaa, R. M. Salem, N. Sandholm, E. E. Schadt, R. A. Scott, L. Stolk, E. E. Vallejo, H.-J. Westra, K. T. Zondervan, P. Amouyel, D. Arveiler, S. J. L. Bakker, J. Beilby, R. N. Bergman, J. Blangero, M. J. Brown, M. Burnier, H. Campbell, A. Chakravarti, P. S. Chines, S. Claudi-Boehm, F. S. Collins, D. C. Crawford, J. Danesh, U. de Faire, E. J. C. de Geus, M. Dörr, R. Erbel, J. G. Eriksson, M. Farrall, E. Ferrannini, J. Ferrières, N. G. Forouhi, T. Forrester, O. H. Franco, R. T. Gansevoort, C. Gieger, V. Gudnason, C. A. Haiman, T. B. Harris, A. T. Hattersley, M. Heliövaara, A. A. Hicks, A. D. Hingorani, W. Hoffmann, A. Hofman, G. Homuth, S. E. Humphries, E. Hyppönen, T. Illig, M.-R. Jarvelin, B. Johansen, P. Jousilahti, A. M. Jula, J. Kaprio, F. Kee, S. M. Keinanen-Kiukaanniemi, J. S. Kooner, C. Kooperberg, P. Kovacs, A. T. Kraja, M. Kumari, K. Kuulasmaa, J. Kuusisto, T. A. Lakka, C. Langenberg, L. Le Marchand, T. Lehtimäki, V. Lyssenko, S. Männistö, A. Marette, T. C. Matise, C. A. McKenzie, B. McKnight, A. W. Musk, S. Möhlenkamp, A. D. Morris, M. Nelis, C. Ohlsson, A. J. Oldehinkel, K. K. Ong, L. J. Palmer, B. W. Penninx, A. Peters, P. P. Pramstaller, O. T. Raitakari, T. Rankinen, D. C. Rao, T. K. Rice, P. M. Ridker, M. D. Ritchie, I. Rudan, V. Salomaa, N. J. Samani, J. Saramies, M. A. Sarzynski, P. E. H. Schwarz, A. R. Shuldiner, J. A. Staessen, V. Steinthorsdottir, R. P. Stolk, K. Strauch, A. Tönjes, A. Tremblay, E. Tremoli, M.-C. Vohl, U. Völker, P. Vollenweider, J. F. Wilson, J. C. Witteman, L. S. Adair, M. Bochud, B. O. Boehm, S. R. Bornstein, C. Bouchard, S. Cauchi, M. J. Caulfield, J. C. Chambers, D. I. Chasman, R. S. Cooper, G. Dedoussis, L. Ferrucci, P. Froguel, H.-J. Grabe, A. Hamsten, J. Hui, K. Hveem, K.-H. Jöckel, M. Kivimaki, D. Kuh, M. Laakso, Y. Liu, W. März, P. B. Munroe, I. Njølstad, B. A. Oostra, C. N. A. Palmer, N. L. Pedersen, M. Perola, L. Pérusse, U. Peters, C. Power, T. Quertermous, R. Rauramaa, F. Rivadeneira, T. E. Saaristo, D. Saleheen, J. Sinisalo, P. E. Slagboom, H. Snieder, T. D. Spector, K. Stefansson, M. Stumvoll, J. Tuomilehto, A. G. Uitterlinden, M. Uusitupa, P. van der Harst, G. Veronesi, M. Walker, N. J. Wareham, H. Watkins, H.-E. Wichmann, G. R. Abecasis, T. L. Assimes, S. I. Berndt, M. Boehnke, I. B. Borecki, P. Deloukas, L. Franke, T. M. Frayling, L. C. Groop, D. J. Hunter, R. C. Kaplan, J. R. O'Connell, L. Qi, D. Schlessinger, D. P. Strachan, U. Thorsteinsdottir, C. M. van Duijn,

C. J. Willer, P. M. Visscher, J. Yang, J. N. Hirschhorn, M. C. Zillikens, M. I. McCarthy, E. K. Speliotes, K. E. North, C. S. Fox, I. Barroso, P. W. Franks, E. Ingelsson, I. M. Heid, R. J. F. Loos, L. A. Cupples, A. P. Morris, C. M. Lindgren, K. L. Mohlke; ADIPOGen Consortium; CARDIOGRAMplusC4D Consortium; CKDGen Consortium; GEFOS Consortium; GENIE Consortium; GLGC; ICBP; International Endogene Consortium; LifeLines Cohort Study; MAGIC Investigators; MuTHER Consortium; PAGE Consortium; ReproGen Consortium, New genetic loci link adipose and insulin biology to body fat distribution. *Nature* **518**, 187–196 (2015). doi:10.1038/nature14132 Medline

75. E. Porcu, M. Medici, G. Pistis, C. B. Volpato, S. G. Wilson, A. R. Cappola, S. D. Bos, J. Deelen, M. den Heijer, R. M. Freathy, J. Lahti, C. Liu, L. M. Lopez, I. M. Nolte, J. R. O'Connell, T. Tanaka, S. Trompet, A. Arnold, S. Bandinelli, M. Beekman, S. Böhringer, S. J. Brown, B. M. Buckley, C. Camaschella, A. J. de Craen, G. Davies, M. C. de Visser, I. Ford, T. Forsen, T. M. Frayling, L. Fugazzola, M. Gögele, A. T. Hattersley, A. R. Hermus, A. Hofman, J. J. Houwing-Duistermaat, R. A. Jensen, E. Kajantie, M. Kloppenburg, E. M. Lim, C. Masciullo, S. Mariotti, C. Minelli, B. D. Mitchell, R. Nagaraja, R. T. Netea-Maier, A. Palotie, L. Persani, M. G. Piras, B. M. Psaty, K. Räikkönen, J. B. Richards, F. Rivadeneira, C. Sala, M. M. Sabra, N. Sattar, B. M. Shields, N. Soranzo, J. M. Starr, D. J. Stott, F. C. Sweep, G. Usala, M. M. van der Klauw, D. van Heemst, A. van Mullem, S. H. Vermeulen, W. E. Visser, J. P. Walsh, R. G. Westendorp, E. Widen, G. Zhai, F. Cucca, I. J. Deary, J. G. Eriksson, L. Ferrucci, C. S. Fox, J. W. Jukema, L. A. Kiemeney, P. P. Pramstaller, D. Schlessinger, A. R. Shuldiner, E. P. Slagboom, A. G. Uitterlinden, B. Vaidya, T. J. Visser, B. H. Wolffenbuttel, I. Meulenbelt, J. I. Rotter, T. D. Spector, A. A. Hicks, D. Toniolo, S. Sanna, R. P. Peeters, S. Naitza, A meta-analysis of thyroid-related traits reveals novel loci and gender-specific differences in the regulation of thyroid function. *PLOS Genet.* **9**, e1003266 (2013). doi:10.1371/journal.pgen.1003266 Medline

76. E. A. Khramtsova, R. Heldman, E. M. Derks, D. Yu, Tourette Syndrome/Obsessive-Compulsive Disorder Working Group of the Psychiatric Genomics Consortium, L. K. Davis, B. E. Stranger, Sex differences in the genetic architecture of obsessive-compulsive disorder. *Am. J. Med. Genet. B. Neuropsychiatr. Genet.* 10.1002/ajmg.b.32687 (2018). doi:10.1002/ajmg.b.32687 Medline

77. E. Y. Kang, C. H. Lee, N. A. Furlotte, J. W. J. Joo, E. Kostem, N. Zaitlen, E. Eskin, B. Han, An Association Mapping Framework To Account for Potential Sex Difference in Genetic Architectures. *Genetics* **209**, 685–698 (2018). Medline

78. M. E. Ritchie, B. Phipson, D. Wu, Y. Hu, C. W. Law, W. Shi, G. K. Smyth, *limma* powers differential expression analyses for RNA-sequencing and microarray studies. *Nucleic Acids Res.* **43**, e47 (2015). doi:10.1093/nar/gkv007 Medline

79. T. L. Bailey, DREME: Motif discovery in transcription factor ChIP-seq data. *Bioinformatics* **27**, 1653–1659 (2011). doi:10.1093/bioinformatics/btr261 Medline

80. R. C. McLeay, T. L. Bailey, Motif Enrichment Analysis: A unified framework and an evaluation on ChIP data. *BMC Bioinformatics* **11**, 165 (2010). doi:10.1186/1471-2105-11-165 Medline

81. S. Naqvi, A. Godfrey, J. Hughes, M. Goodheart, R. Mitchell, D. Page, Conservation, acquisition, and functional impact of sex-biased gene expression in mammalian tissues [Data set], Version 1, Zenodo (2019); http://doi.org/10.5281/zenodo.2658829.

82. A. Dobin, C. A. Davis, F. Schlesinger, J. Drenkow, C. Zaleski, S. Jha, P. Batut, M. Chaisson, T. R. Gingeras, STAR: Ultrafast universal RNA-seq aligner. *Bioinformatics* **29**, 15–21 (2013). doi:10.1093/bioinformatics/bts635 Medline

83. J. F. Hughes, H. Skaletsky, L. G. Brown, T. Pyntikova, T. Graves, R. S. Fulton, S. Dugan, Y. Ding, C. J. Buhay, C. Kremitzki, Q. Wang, H. Shen, M. Holder, D. Villasana, L. V. Nazareth, A. Cree, L. Courtney, J. Veizer, H. Kotkiewicz, T.-J. Cho, N. Koutseva, S. Rozen, D. M. Muzny, W. C. Warren, R. A. Gibbs, R. K. Wilson, D. C. Page, Strict evolutionary conservation followed rapid gene loss on human and rhesus Y chromosomes. *Nature* **483**, 82–86 (2012). doi:10.1038/nature10843 Medline

84. B. Langmead, C. Trapnell, M. Pop, S. L. Salzberg, Ultrafast and memory-efficient alignment of short DNA sequences to the human genome. *Genome Biol.* **10**, R25 (2009). doi:10.1186/gb-2009-10-3-r25 Medline

85. D. Gordon, P. Green, Consed: A graphical editor for next-generation sequencing. *Bioinformatics* **29**, 2936–2937 (2013). doi:10.1093/bioinformatics/btt515 Medline

86. M. Pertea, G. M. Pertea, C. M. Antonescu, T.-C. Chang, J. T. Mendell, S. L. Salzberg, StringTie enables improved reconstruction of a transcriptome from RNA-seq reads. *Nat. Biotechnol.* **33**, 290–295 (2015). doi:10.1038/nbt.3122 Medline

87. R. Patro, G. Duggal, M. I. Love, R. A. Irizarry, C. Kingsford, Salmon provides fast and bias-aware quantification of transcript expression. *Nat. Methods* **14**, 417–419 (2017). doi:10.1038/nmeth.4197 Medline

88. C. Soneson, M. I. Love, M. D. Robinson, Differential analyses for RNA-seq: Transcript-level estimates improve gene-level inferences. *F1000Res.* **4**, 1521 (2015). doi:10.12688/f1000research.7563.2 Medline

89. M. D. Robinson, D. J. McCarthy, G. K. Smyth, edgeR: A Bioconductor package for differential expression analysis of digital gene expression data. *Bioinformatics* **26**, 139–140 (2010). doi:10.1093/bioinformatics/btp616 Medline

90. Y. Zhang, S. A. Sloan, L. E. Clarke, C. Caneda, C. A. Plaza, P. D. Blumenthal, H. Vogel, G. K. Steinberg, M. S. B. Edwards, G. Li, J. A. Duncan 3rd, S. H. Cheshier, L. M. Shuer, E. F. Chang, G. A. Grant, M. G. H. Gephart, B. A. Barres, Purification and characterization of progenitor and mature human astrocytes reveals transcriptional and functional differences with mouse. *Neuron* **89**, 37–53 (2016). doi:10.1016/j.neuron.2015.11.013 Medline

91. P. Reemann, E. Reimann, S. Ilmjärv, O. Porosaar, H. Silm, V. Jaks, E. Vasar, K. Kingo, S. Kõks, Melanocytes in the skin—Comparative whole transcriptome analysis of main skin cell types. *PLOS ONE* **9**, e115717 (2014). doi:10.1371/journal.pone.0115717 Medline

92. C. A. Glastonbury, A. Couto Alves, J. S. El-Sayed Moustafa, K. S. Small, Cell-type heterogeneity in adipose tissue is associated with complex traits and reveals disease-relevant cell-specific eQTLs. *Am. J. Hum. Genet.* **104**, 1013–1024 (2019). doi:10.1016/j.ajhg.2019.03.025 Medline

93. R. Liu, A. Z. Holik, S. Su, N. Jansz, K. Chen, H. S. Leong, M. E. Blewitt, M.-L. Asselin-Labat, G. K. Smyth, M. E. Ritchie, Why weight? Modelling sample and observational level variability improves power in RNA-seq analyses. *Nucleic Acids Res.* **43**, e97 (2015). doi:10.1093/nar/gkv412 Medline

94. J. D. Storey, R. Tibshirani, Statistical significance for genomewide studies. *Proc. Natl. Acad. Sci. U.S.A.* **100**, 9440–9445 (2003). doi:10.1073/pnas.1530509100 Medline

95. B. E. Engelhardt, M. Stephens, Analysis of population structure: A unifying framework and novel methods based on sparse factor analysis. *PLOS Genet.* **6**, e1001117 (2010). doi:10.1371/journal.pgen.1001117 Medline

96. Y. Zhang, K. Klein, A. Sugathan, N. Nassery, A. Dombkowski, U. M. Zanger, D. J. Waxman, Transcriptional profiling of human liver identifies sex-biased genes associated with polygenic dyslipidemia and coronary artery disease. *PLOS ONE* **6**, e23506 (2011). doi:10.1371/journal.pone.0023506 Medline

97. P. Mohammadi, S. E. Castel, A. A. Brown, T. Lappalainen, Quantifying the regulatory effect size of *cis*-acting genetic variation using allelic fold change. *Genome Res.* **27**, 1872–1884 (2017). doi:10.1101/gr.216747.116 Medline

98. B. J. Lesch, S. J. Silber, J. R. McCarrey, D. C. Page, Parallel evolution of male germline epigenetic poising and somatic development in animals. *Nat. Genet.* **48**, 888–894 (2016). doi:10.1038/ng.3591 Medline

99. A. Mathelier, O. Fornes, D. J. Arenillas, C. Y. Chen, G. Denay, J. Lee, W. Shi, C. Shyr, G. Tan, R. Worsley-Hunt, A. W. Zhang, F. Parcy, B. Lenhard, A. Sandelin, W. W. Wasserman, JASPAR 2016: A major expansion and update of the open-access database of transcription factor binding profiles. *Nucleic Acids Res.* **44** (D1), D110–D115 (2016). doi:10.1093/nar/gkv1176 Medline

100. S. Gupta, J. A. Stamatoyannopoulos, T. L. Bailey, W. S. Noble, Quantifying similarity between motifs. *Genome Biol.* **8**, R24 (2007). doi:10.1186/gb-2007-8-2-r24 Medline

101. A. R. Quinlan, I. M. Hall, BEDTools: A flexible suite of utilities for comparing genomic features. *Bioinformatics* **26**, 841–842 (2010). doi:10.1093/bioinformatics/btq033 Medline

102. C. E. Grant, T. L. Bailey, W. S. Noble, FIMO: Scanning for occurrences of a given motif. *Bioinformatics* **27**, 1017–1018 (2011). doi:10.1093/bioinformatics/btr064 Medline

103. W. Dittus, in *Macaque Societies: A Model for the Study of Social Organization*, B. Thierry, M. Singh, W. Kaumanns, Eds. (Cambridge Univ. Press, 2004), pp. 87–112.

104. D. Frynta, J. Baudyšová, P. Hradcová, K. Faltusová, L. Kratochvíl, Allometry of sexual size dimorphism in domestic dog. *PLOS ONE* **7**, e46125 (2012). doi:10.1371/journal.pone.0046125 Medline

105. S. Gregorová, P. Divina, R. Storchova, Z. Trachtulec, V. Fotopulosova, K. L. Svenson, L. R. Donahue, B. Paigen, J. Forejt, Mouse consomic strains: Exploiting genetic divergence between *Mus m. musculus* and *Mus m. domesticus* subspecies. *Genome Res.* **18**, 509–515 (2008). doi:10.1101/gr.7160508 Medline

106. F. H. Porter, F. Costa, G. Rodrigues, H. Farias, M. Cunha, G. E. Glass, M. G. Reis, A. I. Ko, J. E. Childs, Morphometric and demographic differences between tropical and temperate Norway rats (*Rattus norvegicus*). *J. Mammal.* **96**, 317–323 (2015). doi:10.1093/jmammal/gyv033